AFFINITY LIGAND BIOSENSING LIQUID MEMBRANES

by

Martin Charles Wiles

A thesis submitted for the degree of

MASTER OF PHILOSOPHY

Department of Chemistry

October, 1985

University of Southampton

ABSTRACT

The technique of d-c polarography was developed for a water/1,2 dichloroethane system and it was shown that analysis of results can follow in an analogous manner to those obtained at a dropping mercury electrode.

The suitability of the triazine dyes Cibacron blue F3GA and Procion blue Mx-R as biosensing ligands in a liquid-liquid system was investigated using cyclic voltammetry and interfacial tension. The latter made use of the process of video image processing and demonstrated a strong adsorption/desorption phenomenon of the dyes. This phenomenon is explained in terms of the ionization of the NH_2 group of the antracene part of the dyes forming a zwitterion which is strongly adsorbed. It is proposed that only the anthracene part of the dye molecule is in contact with the aqueous phase by virtue of its polarity.

CONTENTS

CHAPTER 1

1.1   Objectives of the Work

The aim of the project was to assess the possibility of combining the recent developments in dye-ligand affinity chromatography with those obtained in the studies of liquid-liquid interfaces and possibly therefore to develop a biosensing technique for proteins.

It has been found that a number of dyes (1-4) and particularly those of the triazine group (5,6) will bind a large variety of proteins with varying degrees of specificity (5,6). Some of the dyes such as Cibracron blue F3GA (a monochlorotriazine) have a rather broad specificity; however, dyes of greater specificity also exist (6,7,8).

The dyes used in this study were Procion blue MX-R and Cibracron blue F3GA, both triazines. The Cibracron blue F3GA (CBA) was chosen because of the extensive use of this dye in affinity chromatography protein purification, since the discovery by Kopperschläger et al (9,10) that some proteins bound to blue Dextran. Blue Dextran is a void volume marker in gel permeation chromatography and CBA is its chromophore. CBA has been shown to be the protein binding part of the Dextran molecule (10). CBA has a tendency to bind dehydrogenases (5) and kinases (5) but has been shown to bind to a number of other proteins of different type (see (5)). CBA has also been studied with respect to its possible use as a structural probe (10,11) and therefore the nature of the dye-protein interaction for a few proteins has been investigated.

Procion blue MX-R was chosen as the second dye for investigation in order to compare a dichlorotriazine to a monochlorotriazine dye, the similarities in structure still remaining sufficiently close to allow for a sensible comparison (Fig.1.1). Procion blue MX-R is also used

CIBACRON BLUE F3GA

PROCION BLUE MX-R

Figure 1.1   The structures of the triazine dyes used in this study

in affinity chromatography for protein purification (12).

The formation of a dye-protein complex appears to be particularly suited to investigation by electrochemical means using liquid-liquid interfaces.

Liquid-liquid interfaces formed from two immiscible electrolyte solutions (ITIES) have been suggested as a model for a membrane (13) and work has been carried out in order to understand the distribution of potential across the interface and its polarization characteristics. as well as the effect of biological materials on the interfacial properties. Some recent work with phospholipids (14-16) which demonstrated their adsorption and coverage to be potential dependent, led to the idea of modifying the dye molecules by the addition of long hydrocarbon chains. It was hoped that this would create both a very hydrophobic moiety which could interact strongly with the organic phase and anchor the dye molecules at the interface and a more hydrophilic moiety which could be free to interact with proteins in the aqueous phase.

To study these dyes it was proposed to use the techniques of the electrolyte dropping electrode (17-20) and cyclic voltammetry. For the study of adsorption and desorption phenomena at the interface it was proposed to use measurements of interfacial tension via the technique of video image processing (21,22).

1.2   Introduction

1.2.1. Affinity dyes

Dyes were used in this work because of their demonstrated binding to proteins in affinity chromatography (see (5)). (Affinity chromatography is a technique which utilises the affinity of particular chemical groups for specific proteins). The first example of affinity chromatography was Starkenstein's immobilisation of amylase with starch as substrate (23). The method was, however, not fully appreciated as a method of protein purification until 1968 when inert supports and methods of ligand attachment were developed. It was also at this time that group-specific ligands i.e. ligands which were used for a group of proteins rather than a specific protein, were realised as a more practicable, cheaper alternative to specific ligands e.g. NAD (nicotinamide adenine dinucleotide) and cAMP (cyclic adenosine monophosphate). The group-specific ligands did not however overcome all the problems of affinity chromatography and once it was known that certain dyes could perform a similar function to co-factors, their popularity particularly for large scale preparations, increased.

Some of the advantages in the use of dyes arise from their ease of matrix attachment, higher capacities, cheapness, reuseability and their long storage times.

The first dye to find application in affinity chromatography was Cibracron blue F3GA (CBA). This arose from the discovery that Blue Dextran, when used as a void volume marker in gel permeation chromatography bound phosphofructokinase (9,10) and pyruvate kinase (24). It was found that CBA was the chromophore and protein binding part of blue Dextran (10).

The triazine dyes, which were originally used in the textile
industry and are based on cyanuric chloride (trichloro-s-triazine)
have been found since to be useful to varying degrees for protein
purification, e.g. Procion Red HE-3B has a higher affinity than CBA
for NADP dependent dehydrogenases and reduced affinity for NAD-
dependent dehydrogenases. Three other triazine dyes used are Orange
A, Green A, and Blue B (Fig.1.2), all developed recently by Amicon
(6). Orange A binds very few proteins i.e. approximately 5% in an
extract where CBA binds 30-60% of proteins present. It binds rabbit
muscle malate dehydrogenase, rat liver lactate dehydrogenase, pig
heart citrate synthetase as examples. In contrast with Orange A, Green
A will bind a very large number of proteins and is very specific for
glyceraldehyde-3-phosphate dehydrogenase and almost quantitative
separations can be achieved. Blue B is similar to Orange A; it has an
unusual phthalocyanine chromophore and it binds well phosphoglycerate
kinase, 6-phosphogluconate dehydrogenase and malate dehydrogenase.

Dyes are easily detected in a free and in a bound state to
proteins and are therefore useful in studies using probes of protein
structure (1-4). The widespread use of triazine dyes in protein
purification has led to interest in the nature of the dye-protein
interactions, and the possibility of their use as structural probes has
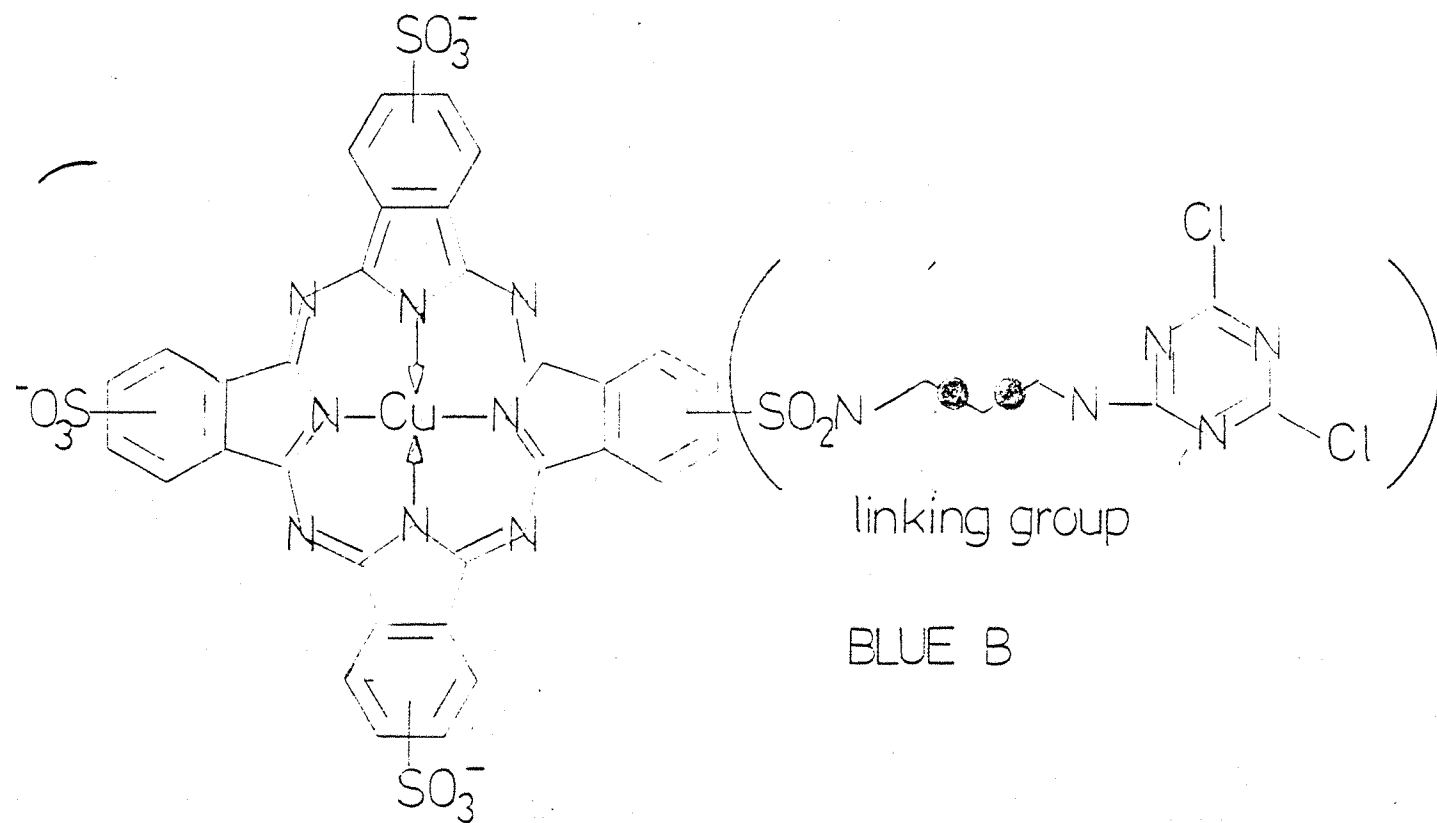been explored (10,11).

As mentioned previously, CBA-protein specificity was first noticed
in experiments with phosphofructokinase (9,10) and pyruvate kinase (24)
when it was found that it required only low concentrations of substrates
or effectors to cause the dissociation of the dye from the protein.
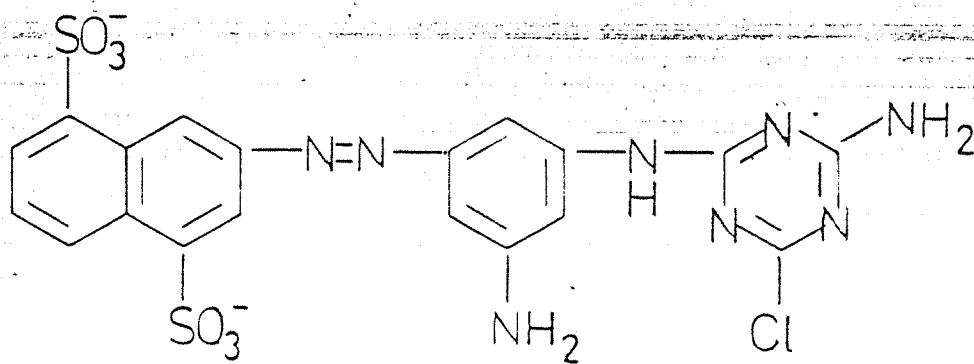
ORANGE A

GREEN A

BLUE B

linking group
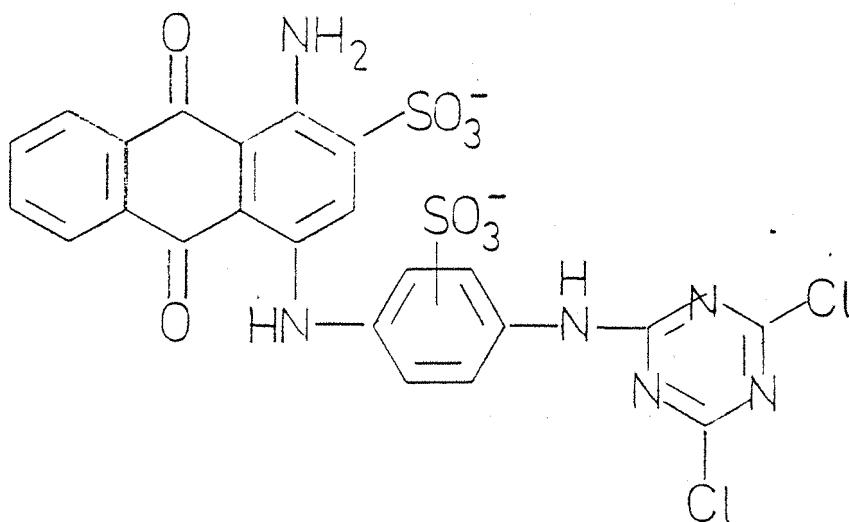
Figure 1.2   The structures of some triazine dyes which are used
             in affinity chromatography.

Kopperschläger et al (9) eluted yeast phosphofructokinase from blue

Dextran with 2-2.5 mM ATP and Blume et al (25) could dissociate the

dye-protein complex with low concentrations of fructose 1,6-diphosphate.

Böhme et al (10) observed that Cibracron Brilliant blue FBR-P did not

bind yeast phosphofructokinase and concluded that the 1-amino group of

the anthraquinone and the 2'-sulphonic acid residue of the phenylene-

diamine ring were responsible for the high specificity of the dye-

phosphofructokinase interaction. This part of the dye showed distinct

similarities to an ATP molecule, i.e. shape, aromaticity and charge

distribution. Coupled with this, the knowledge that ATP could dissociate

dye-protein complex competitively led to the suggestion that the dye was

a structural analogue of ATP (10).

After this suggestion a large number of workers further studied

the dye-protein interaction using kinetic (26-31), spectrophotometric

(26,27,11) and chromatographic techniques (26-30). It was found that

CBA bound most NAD and NADP dependent dehydrogenases and many ATP

dependent enzymes with competitive loss of their activity. The dye-

protein complexes could be cleaved non-specifically by high salt

concentration or low specific ligand concentration (nucleotide ligand).

The binding of the dye to an obviously hydrophobic region could be

determined from the perturbation of the dyes visible spectrum.

The information allowed Thompson et al (28) to suggest that CBA

mimicked the conformation of NAD and therefore bound to the super-

secondary structural unit of the dinucleotide fold. This fold consists

of a β-sheet core of 5/6 parallel strands flanked above and below by

stabilising α-helical loops. The amino acids in this region are apolar

in character and therefore the whole structure forms a hydrophobic

pocket in which the nucleotide binds.

Stellwagen et al (11) further suggested that provided a protein bound CBA and was dissociated with substrate or effector chromatography on blue Dextran could be used to predict the presence of a dinucleotide fold in a protein. This suggestion, however, when applied to aldolase which was predicted to have a substrate binding site very similar to the NAD domain (32) and hence a model enzyme for testing the hypothesis, did not work. Further, Grazi et al (33) found that aldolase bound three molecules of dye/aldolase subunit and that ATP and 1,6 biphosphate could compete with the dye. The dye does not bind to the catalytic sites and therefore it is unlikely that a 40,000 MW subunit should have three dinucleotide folds.

Studies with the dye Procion Red HE-3B (34) added to the belief that CBA was not a NAD specific analogue. Procion Red, despite its notable structural difference, interacts with all enzymes binding CBA e.g. (35). Procion Red HE-3B appears to exhibit the same competitive inhibition of dehydrogenases and kinases as CBA.

Edwards and Woody (36) studied the interaction of CBA with the four dehydrogenases, lactate, alcohol, cytoplasmic malate and glyceraldehyde-3-phosphate by circular dichroism and compared this interaction with that of the dye Congo Red. They concluded that dyes were not highly specific analogues of co-factors. They suggested that the reasons for the interaction was due to the several types of functional group and conformational freedom of the dye molecule which allowed the insertion of aromatic rings into hydrophobic pockets while other parts of the molecule moved to minimize unfavourable interactions. They state, however, that due to limitations on conformational freedom in the dye molecule and the

enzyme active site some specificity is achieved. CBA has also been found to interact with proteins which are known to be devoid of the dinucleotide fold; such examples are albumin (37), trypsin (5), L-arabinose binding protein in E. Coli (5) and this finally led to the disproof of Stellwagen's hypothesis.

However, in disproving Stellwagen's hypothesis it has not been disproved that the dye cannot bind to the dinucleotide fold and Biellmann et al (38) have in fact demonstrated via X-ray crystallography of alcohol dehydrogenase that CBA is in fact bound at this fold in this enzyme. The x-ray data does support however the work of Bohme et al (10) and Beissner and Rudolph (39). In this case the 1-amino-4(4'-aminophenylamino)-anthraquinone-3,4'-disulphonic acid dye portion is responsible for the dinucleotide fold interaction. Apparently, from kinetic experiments on dehydrogenases and kinases, this has also been concluded by Bornmann and Hess.

The dyes can also bind to proteins via non-specific interactions as the ionic groups can act as weak ion-exchangers. To distinguish between specific and non specific interactions the effect of pH and substrate/effector concentration can be determined.

In the present view of triazine dye-protein interaction, a hydrophobic area on the surface of a protein which is surrounded by hydrophilic residue is required and as suggested by Glazer in 1970 (40) for uncharged aromatic dyes this occurs generally in areas which overlap natural ligand binding sites, although this is not essential. The interaction is both hydrophobic and electrostatic, although the latter is more concerned with the stability of the complex once formed i.e. if ionic groups match those on the protein a stronger interaction results.

It is the aromaticity which leads to the hydrophobic binding and therefore in principle all ionic aromatic compounds should bind proteins with hydrophobic pockets. However, any kind of specificity must arise from the size of the aromatic molecule and the size of the hydrophobic region available for binding. It would appear that for CBA the 1-amino 4(-4'-aminophenylamino)-anthraquinone 2,3' sulphonic acid part of the molecule is the part which binds to the dinucleotide fold but the dinucleotide fold is only a special case of dye binding.

It is unfortunate that what originally appeared an excellent group specific ligand has not fulfilled expectations. However, with increasing research, it should be possible to make dyes more and more specific as has already been demonstrated (7,6) or to predict which proteins will bind.

1.2.2. The Interface between two Immiscible Electrolyte Solutions (ITIES)

The first experiment carried out at an ITIES was that of Nernst and Reisenfeld in 1902 (41). These authors found that the passage of current through the water-phenol interface obeyed a transport equation according to:

$$j(t_+^w - t_+^o)F = - D_w \left(\frac{\delta C_w}{\delta_x} \Big|_{x=0} + D_o \frac{\delta C_v}{\delta_x} \Big|_{x=0} \right)$$

where j = current density, t = transport number, D = diffusion coefficient, x = interface position. Sand had derived a similar relation for systems having an excess of supporting electrolyte (42). These early experiments measured only the transport number of hydrophobic ions in the oil phase.

It was not until 1956 that non-equilibrium conditions were investigated; Gustalla (43) investigated the system acetyltrimethyl-ammonium bromide in water-nitrobenzene and a change in interfacial tension when current was passing was observed.

This phenomenon was named "electroadsorption". Similar systems were also studied by other researchers and finally Blank (44) showed that electroadsorption could be understood in terms of accumulation and depletion of surface active species at the interface.

The properties of the electrical double layer at the ITIES have been studied by Gavach et al (45) and this work led in 1977 to an interfacial model postulating the existence of compact layers similar to those observed at the metal-electrolyte interface. However, more recent work by Samec et al (46,47) and Reid et al (48,49) have shown that the potential drop across the proposed compact layers is very close to zero and remains thus even when the potential difference between the phases is altered. Samec et al (46,47) used impedence measurements of interfacial capacitance of water-nitrobenzene and Reid et al (48,49) used interfacial tension to obtain electrocapillary curves as well as differential capacitance of the water-nitrobenzene interface. The results were in agreement with each other.

Girault et al (50,51) have also measured liquid-liquid interfacial tension (method described later) (21,22) and they suggested that both mixed solvation and interfacial ion pairing accounts for the absence of clearly defined inner layers. Girault et al further investigated impedance and the surface tension at the water-1,2 dichloroethane interface in the presence of phospholipids (16). The results were in disagreement with a "back to back" diffuse double layer and strong adsorption effects were observed.

The relationship of current to applied potential was first investigated by Guastalla (52) but was more extensively investigated by

Gavach et al (45,53) who measured steady-state polarization curves using chronopotentiometry. In these studies chronopotentiograms similar to those for the metal-electrolyte interfaces were observed and this analogy has been demonstrated by a number of different techniques. However, Melroy et al (54) have outlined some important differences:

i) Diffusion-migration via Nernst-Planck equation rather than Ficks 1st law must be considered.

ii) Interfacial transport of ions of opposite sign must be considered because of salt partition equilibria, and

iii) Partition equilibria is a non-linear ionic process that can lead to insoluble equations.

The techniques used to study the ITIES are chronopotentiometry (55, 56,53,57), electrolyte dropping electrode (17-20, 58,59,60), cyclic voltammetry (53,13,61), impedence (46,47,16) and differential pulse stripping voltammetry (62). The organic phase has also been varied and other solvents besides nitrobenzene and 1,2 dichloroethane have been studied. These are propiophenone (63), 4-isopropyl-1-methyl-2-nitrobenzene (64), dichloromethane (65), 4-methyl-2-pentanone (66) and hexone (67).

A wide variety of ion transfers have also been studied (59,55,68) and facilitated transport via valinomycin (61), macrocyclic polyethers (69) etc. has also been investigated.

The applications of liquid-liquid interfaces are very wide covering areas in biology to material science. The direction of this study is towards electronalaytical biochemistry.

CHAPTER 2

2.1 Theory of Interface of Two Immiscible Electrolyte Solutions

If we consider a system of two immiscible solvents α and β which contain a common ion B^+, the Galvani potential difference is determined by the Nernst-Donnan equation:

$$\Delta_\alpha^\beta \psi = \left[\mu_{B_1^+}^o (\alpha) - \mu_{B_1^+}^o (\beta) \right]/F + \frac{RT}{zF} \ln \frac{a_{B^+} (\alpha)}{a_{B^+} (\beta)} \tag{1}$$

$$= \Delta G_{tr_{B^+}}^{\alpha \to \beta} /F + \frac{RT}{zF} \ln \frac{a_{B^+} (\alpha)}{a_{B^+} (\beta)} \tag{2}$$

where μ^o = standard chemical potential, z = the ionic charge, a = activity and $\Delta G_{tr_{B^+}}^{\alpha \to \beta}$ is the free energy of transfer of ion B^+ from α to β and is considered for low concentrations to be the difference in free energies of solvation of B^+ in both phases.

As $\Delta G_{tr}^{\alpha \to \beta}$ is not obtainable for the individual ions but for the neutral salt only an extra-thermodynamic assumption is necessary to allow for a quantitative determination of free energy of transfer for individual ions. The most often used assumption is the "TATB" assumption (70) which states that the anion and cation of tetraphenylarsonium tetraphenylborate (TPAs TPB) have equal values of $\Delta G_{tr}^{\alpha \to \beta}$, for any solvents. This assumption is based on the identity of the ionic radii for the anion and cation of this salt.

It follows that the standard electrical potential difference between two immiscible phases can be determined from an ion (i) of charge z by:

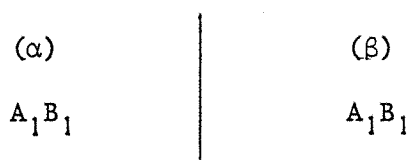$$\Delta_\alpha^\beta \psi_i^o = - \Delta G_{tr,i}^{\alpha \to \beta} / zF \tag{3}$$

Several different cases can be considered:

(I) Single electrolyte partition - for a single electrolyte distributed between two immiscible phases (Scheme A) then $\Delta_\alpha^\beta \psi$ will be given by:
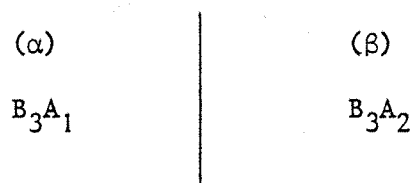
$$\Delta_\alpha^\beta \psi^o = \tfrac{1}{2}(\Delta G^o_{tr_{A,}{}^-}{}^{\alpha\to\beta} - \Delta G^o_{trB,}{}^+{}^{\alpha\to\beta})\qquad (4)$$

Scheme A

(α)	(β)
A_1B_1	A_1B_1

When there is a large difference in the absolute values of free energies of transfer between the ions the potential difference will be determined by the ion having the largest value of $\Delta G^o_{tr}{}^{\alpha\to\beta}$.

(II) Single ion partition - A more often studied situation is that shown in Scheme B.

(α)	(β)	
B_3A_1	B_3A_2	Scheme B

here the ion common to both phases $B_3{}^+$ is more easily transferred than $A_1{}^-$ and $A_2{}^-$ from α to β and β to α respectively, i.e.

$$\Delta G^o_{tr_{A_1}{}^-}{}^{\alpha\to\beta} >> 0 \qquad (5)$$

$$\Delta G^{o\,\alpha\to\beta}_{tr_{A_2}{}^-} << 0 \qquad (6)$$

$$\Delta G^o_{tr,A_2{}^-}{}^{\alpha\to\beta} << \Delta G^o_{tr,B_3{}^+}{}^{\alpha\to\beta} << \Delta G^o_{tr,A_1{}^-}{}^{\alpha\to\beta} \qquad (7)$$

The value of $\Delta_\alpha^\beta \psi$ here is determined both by $\Delta G_{tr}^{\alpha \to \beta}$ and the activities

of B_3^+ in α and β from equations (1) and (2). The activities of $A_1^-(\beta)$
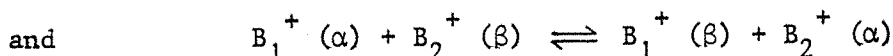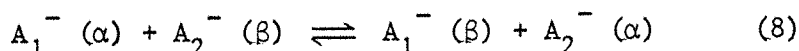
and A_2^- (α) are considered to be very small.

III - Polarised interfaces - Scheme C shows the situation when the

electrolytes are restricted completely in their respective phases

Scheme C

(α)	(β)
A_1B_1	A_2B_2
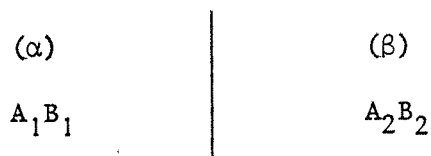
This condition is satisfied if $\Delta G^o{}_{tr,A_1B_1}^{\alpha \to \beta}$ and $\Delta G^o{}_{tr,A_2B_2}^{\beta \to \alpha}$ are large and

positive.

In consequence, the equilibria

$$A_1^- \ (\alpha) + A_2^- \ (\beta) \rightleftharpoons A_1^- \ (\beta) + A_2^- \ (\alpha) \qquad (8)$$

and $\qquad B_1^+ \ (\alpha) + B_2^+ \ (\beta) \rightleftharpoons B_1^+ \ (\beta) + B_2^+ \ (\alpha)$

are very far to the left hand side. $\Delta_\alpha^\beta \psi$ can be varied independently

of the composition and the interface is termed polarized.

If we now consider the above situation with the addition of an

electrolyte B_3A_1 to (α) and B_3A_2 to (β) in low concentration with respect

to A_1B_1 and A_2B_2, then A_1B_1 and A_2B_2 will act as base electrolytes and

if B_3^+ has characteristics as before the external input of $\Delta V = \Delta\psi_{eq} + \eta$

will lead to the transfer of B_3^+ ion across the interface.

In all the electrochemical experiments described in this work, base

electrolytes have been used.

2.2　POLAROGRAPHY WITH AN ELECTROLYTE DROPPING ELECTRODE

2.2.1 Introduction

The principles and invention of polarography are attributed to Professor J. Heyrovsky of Prague at around the time of 1925. He used mercury to form a drop which issued from a small capillary and dropped under the effect of gravity. It was not until 1976 that Koryta (17) applied the same principles to develop the rising electrolyte dropping electrode using an ITIES. He obtained polarograms with a S-shape denoting ion transfer and found the limiting current for TMA$^+$ (tetramethylammonium ion) to be proportional to the concentration of the ion.

Since that time current scan polarography has been introduced for the study of the transfer of 1,10-phenanthroline and its derivatives (68) and of TMA$^+$ (60). More recently still a.c. polarography has been used by Osaki et al (58) to study TMA$^+$ transfer.

In this study d.c. polarography was developed.

2.2.2 Experimental

The assembly of the electrolyte dropping electrode (EDE) is shown in Fig.2.1. The reservoir contained the base electrolyte 0.05M LiCl(BDH) in triply distilled water and the drop ascended through Analar 1,2-dichloroethane (BDH) containing 10^{-3}M TBATPB. The TBATPB was made by precipitation from NaTPB (Fluka) and TBACl (Fluka) and twice recrystallized from acetone (TEATPB was made similarly from TEACl (Eastman)).

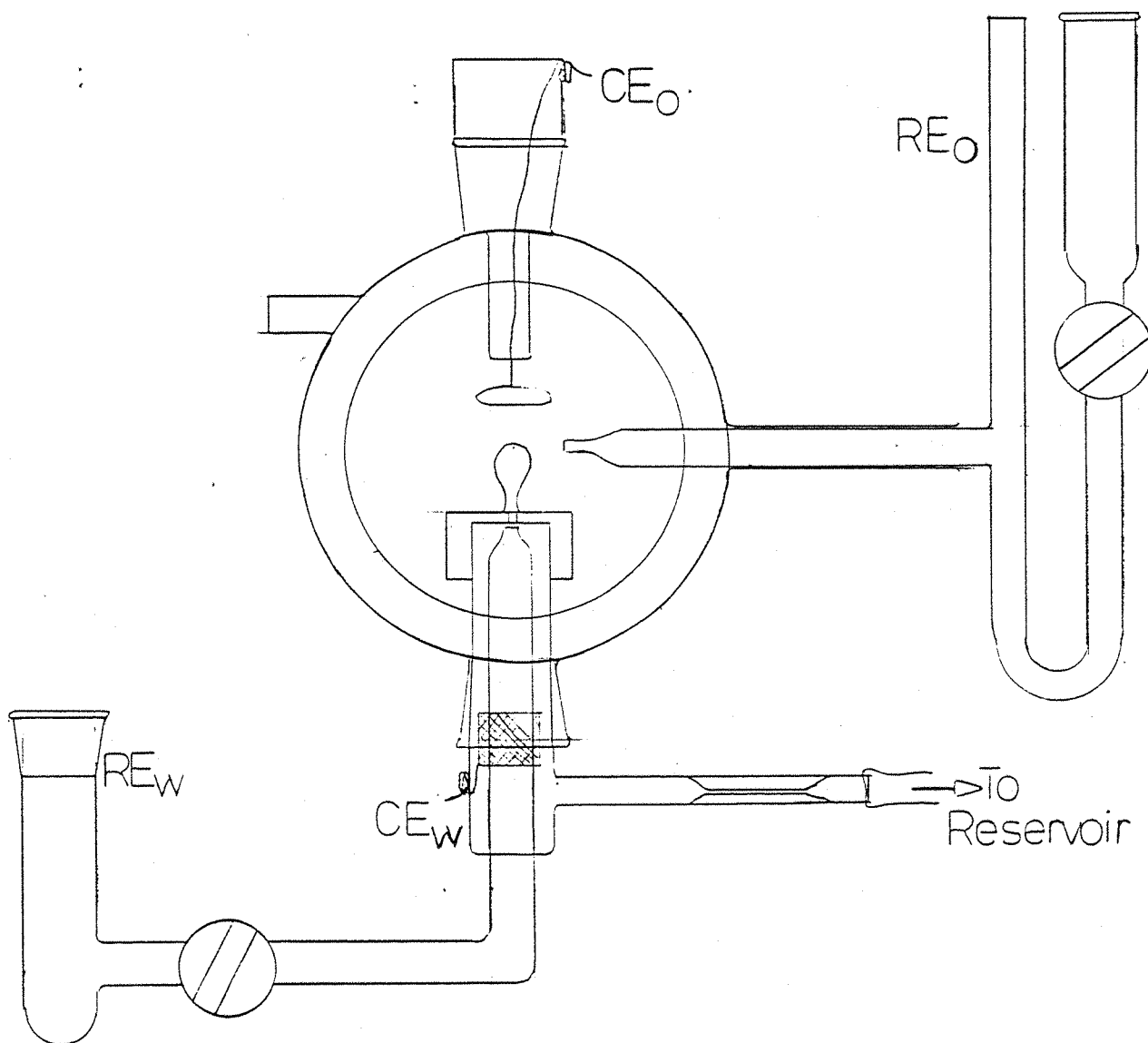All solutions were equilibrated with each other before use.

Figure 2.1 The cell design used for the measurement of polarograms.

The potential was applied via a four electrode potentiostat with positive feedback for automatic ohmic potential drop compensation. The reference electrodes used were standard calomel electrodes.

The instantaneous I-t curves were stored on a Gould 3500 digital storage oscilloscope and recorded on a Bryans 26000 X-Y chart recorder which was also used to record the polarograms.

2.2.3. Results

Fig. 2.2 shows a typical polarogram of the base electrolytes and Fig.2.3 that of a polarogram in the presence of 60 μM TEATPB in the organic phase. The wave at approximately -275 mV corresponds to the to the transfer of the TEA$^+$ ion from the organic to the water phase. Occasionally and particularly at low concentrations of the ion under study, a polarographic maximum was present (Fig.2.4). This has been accounted for previously (19) by the tangential motion of the electrolyte at the surface of the drop and is a well known effect in polarography.

2.2.4. Discussion

The currents observed for the base electrolytes can be due to double layer charging effects and/or ion transfer across the interface. In principle it should be possible to distinguish between these from the analysis of the current-time transients since capacitative currents depend on the time derivative of the drop area whereas kinetic and diffusional currents have a direct dependence on the drop area.
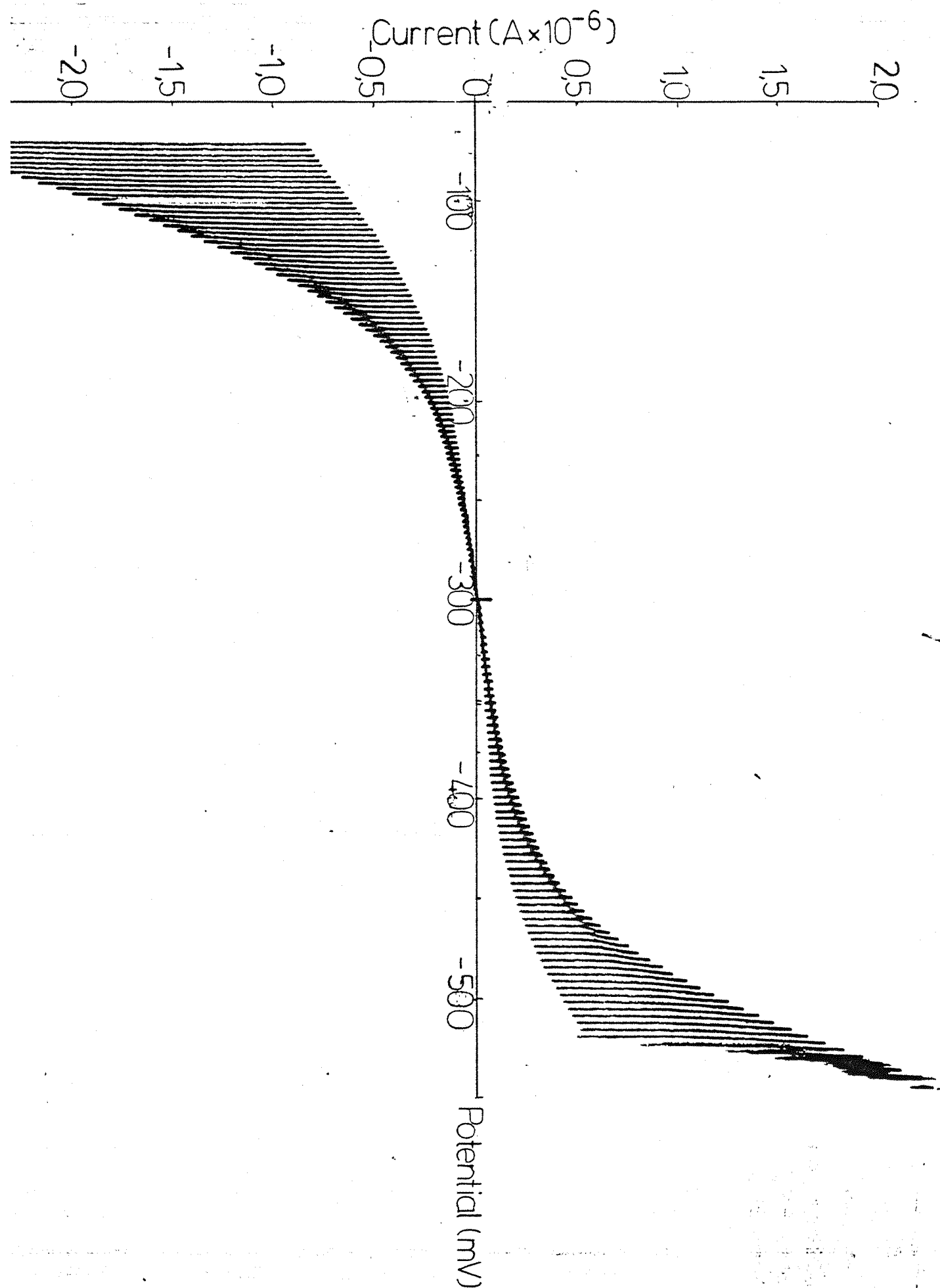
Figure 2.2 Polarogram of base electrolytes (LiCl 0.05M(aq) and TBATPB 10^{-3}M(org)). Scan rate = 1mV/s. Droptime = 3.2 sec.
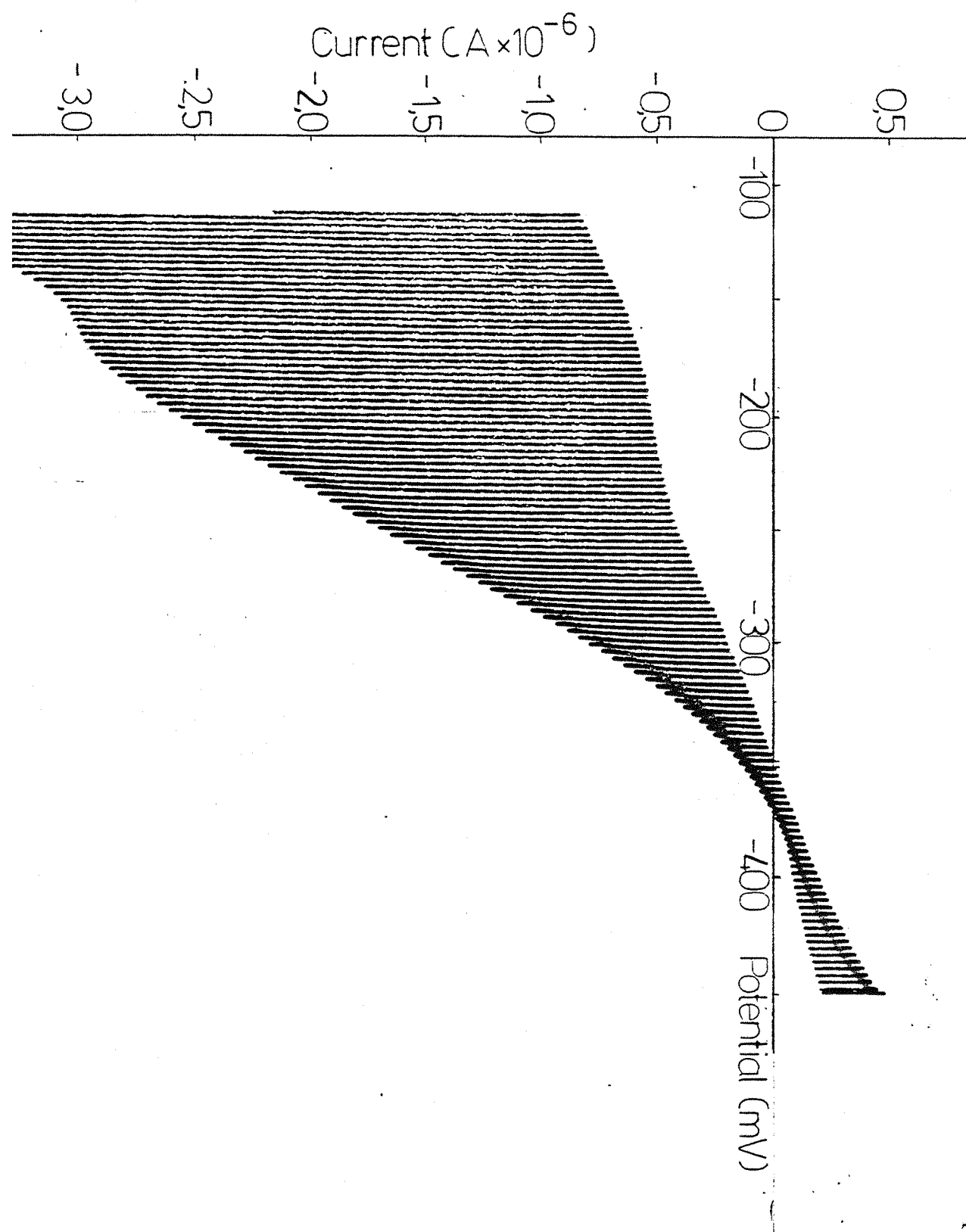
Figure 2.3   Polarogram of 60μM TEA $^+$ transfer. (Base electrolytes LiCl 0.05M(aq) and TBATPB 10^{-3} M(org) Scan rate = 1mV/s Droptime = 3.0 sec.
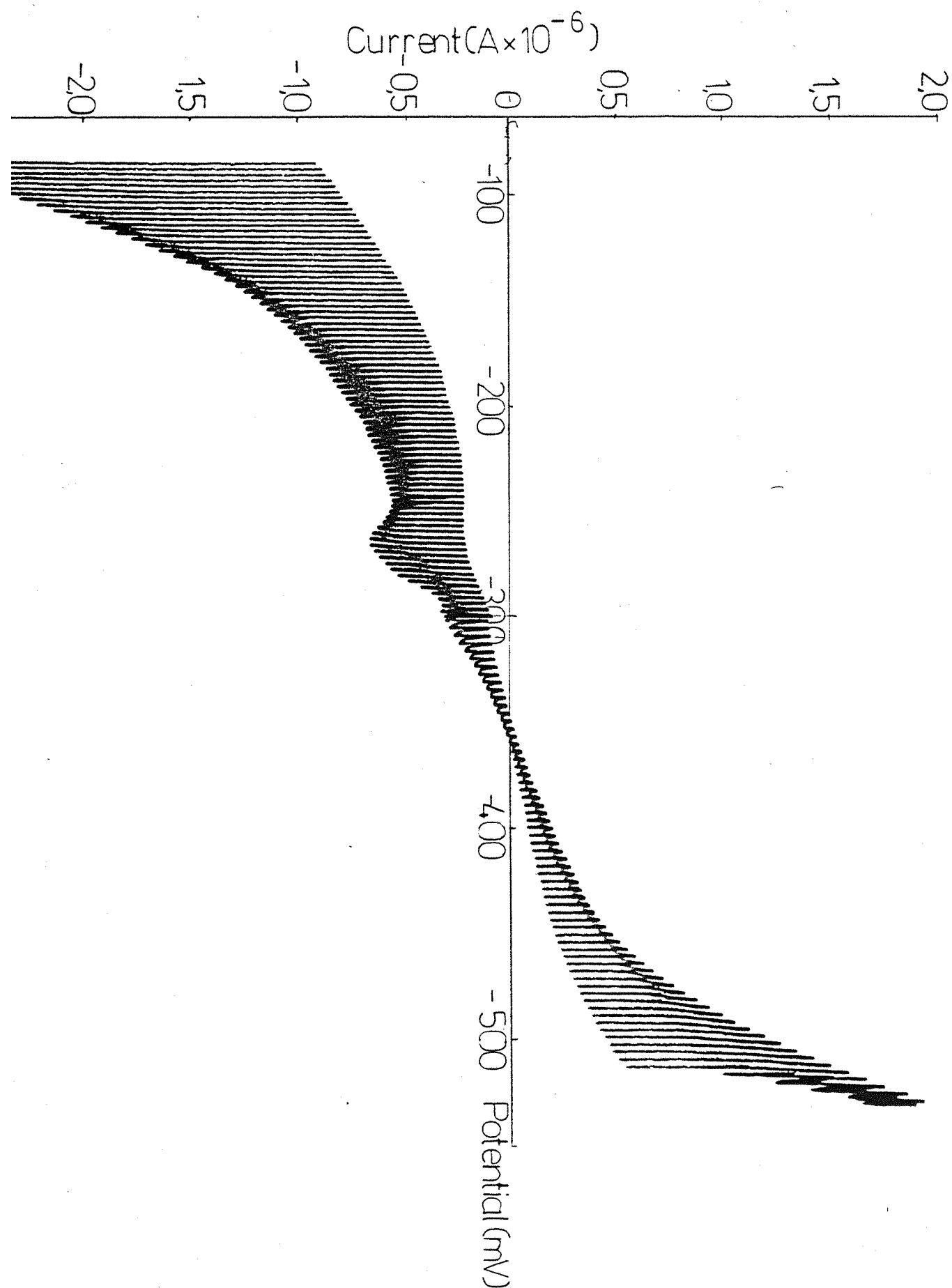
Figure 2.4   Polarogram of 10µM TEA$^+$ transfer demonstrating a polarographic maxima. (Base electrolyte LiCl 0.05M(aq) and TBATPB 10^{-3}M(org) Droptime = 3.2 sec. and scan rate = 1mV/s.
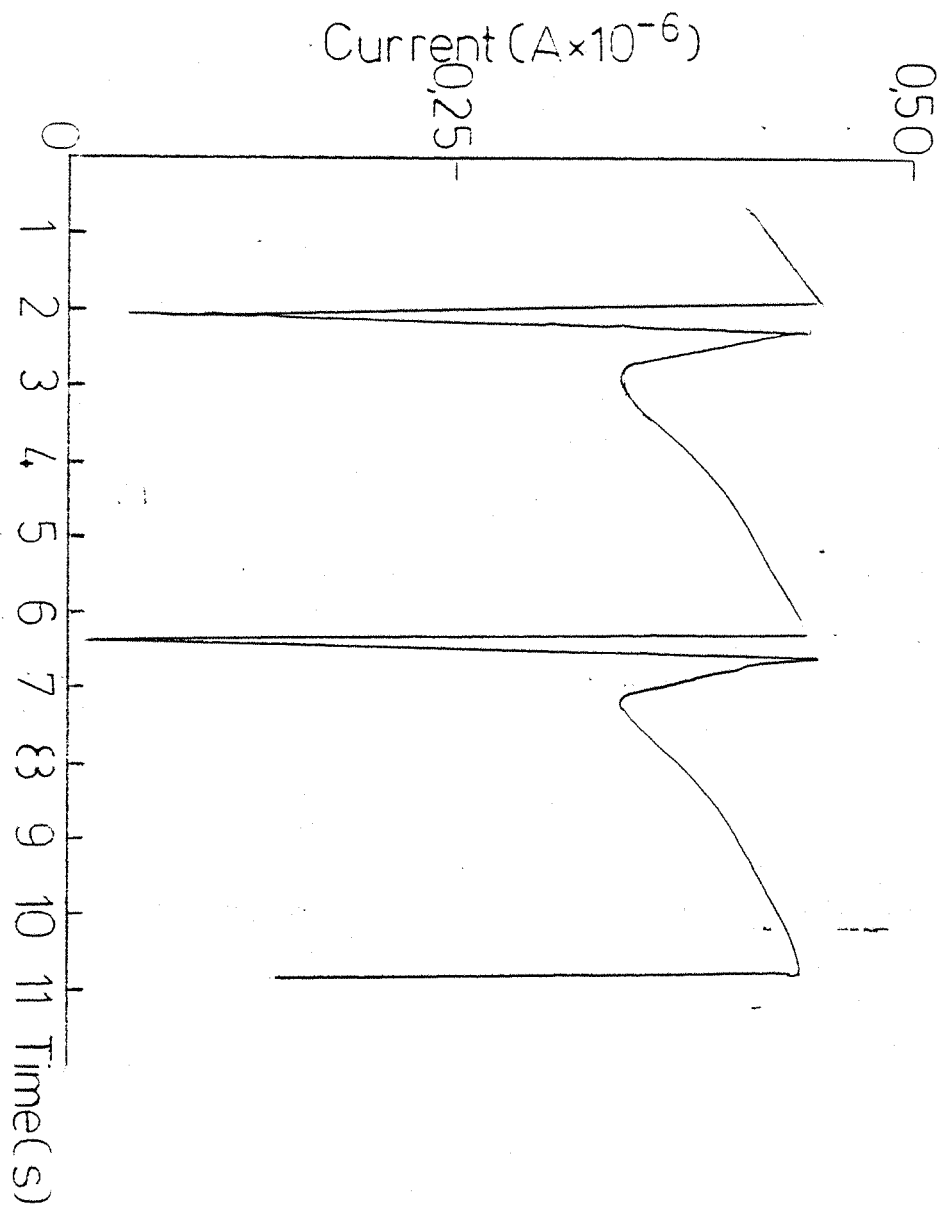
Figure 2.5   Instantaneous current-time profile for base electrolytes NaCl
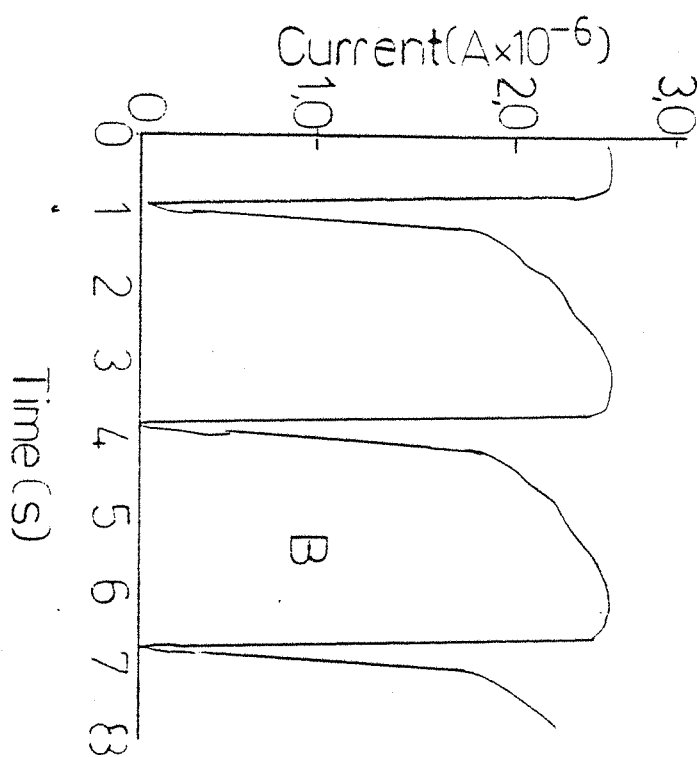0.05M(aq) and TBATPB 10^{-3}M(org) at an applied potential of
Eapp = 450mV.

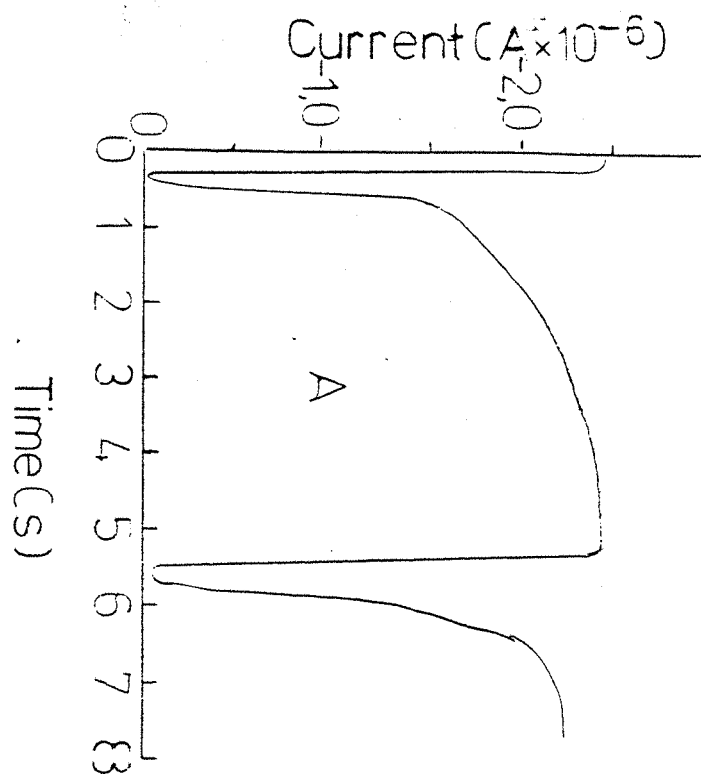Figure 2.6   Instantaneous current-time profiles for TEA$^+$ transfer at Eapp = 200mV
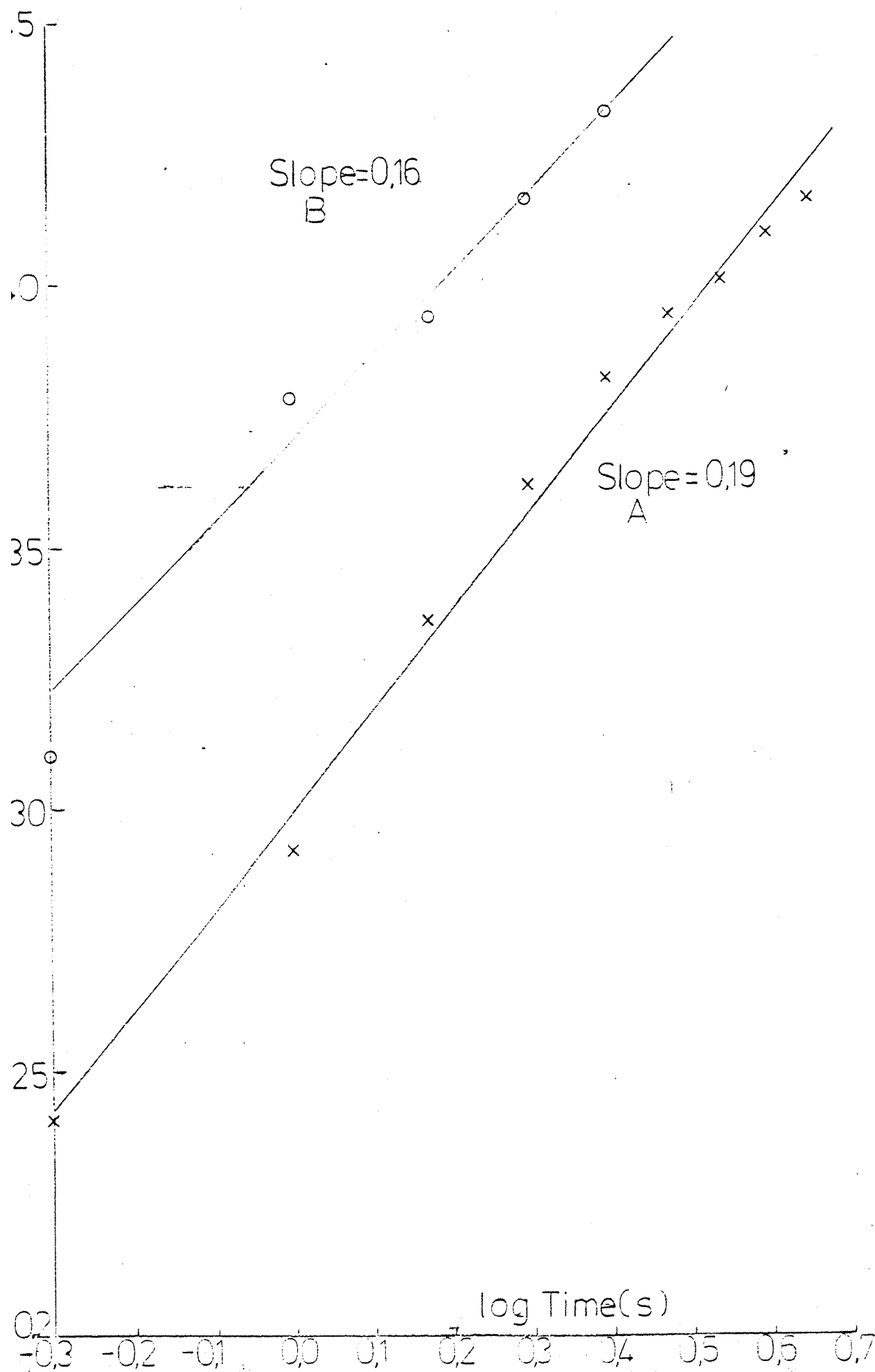Base electrolyte is LiCl 0.05M(aq) and TBATPB 10^{-3}M(org).

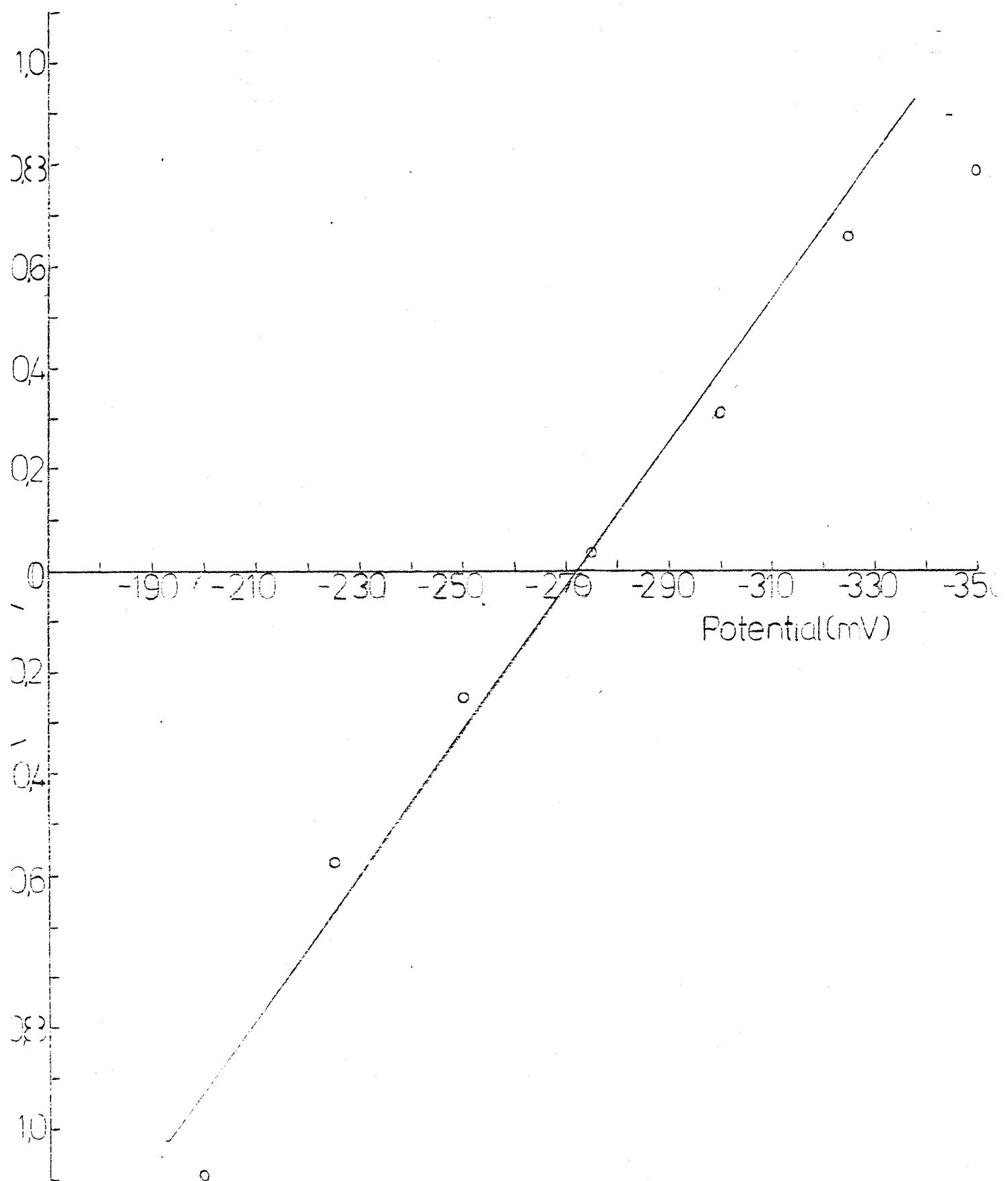Figure 2.7 The logarithmic analysis of the current-time profiles of drops A and B of Figure 2.6.

Figure 2.8 Logarithmic analysis of the polarographic wave for the transfer of 60μM TEA $^+$. Base electrolytes LiCl 0.05M(aq) and TBATPB 10^{-3}M(org).

Fig. 2.5 shows an instantaneous I-t drop profile for the base electrolyte. The presence of a current minimum indicates a combination of double layer charging currents and ion transfer.

If we consider purely capacitative effects, the current (i_c) is given by:

$$i_c = C\Delta E \frac{dA}{dt} \qquad (9)$$

where C = integral capacitance, ΔE = difference in potential between the potential of zero charge (E_{pzc}) and the applied potential, and A = area.

Considering the flow rate, m is uniform throughout the drop life as a reasonable first approximation, the change of radius of a drop as a function of time is:

$$r(t) = (\frac{3}{4\pi})^{1/3} \cdot \frac{m^{1/3}}{\eta^{1/3}} t^{1/3} \qquad (10)$$

and therefore:

$$A(t) = 4\pi (\frac{3}{4\pi})^{2/3} \frac{m^{2/3}}{\eta^{2/3}} t^{2/3}$$

$$= \frac{4.836}{\eta^{2/3}} m^{2/3} t^{2/3} \qquad (11)$$

hence

$$i_c(t) = C\Delta E \frac{4.836}{\eta^{2/3}} m^{2/3} t^{-1/3} \qquad (12)$$

For a purely diffusionally controlled ion transfer process the current is given by: (71)

$$i(f) = \frac{4.022 \times 10^5}{\eta^{2/3}} zD^{1/2}C^o m^{2/3} t^{1/6} \qquad (13)$$

where C^o is the surface concentration of the species being transferred.

The total current , i_T is:

$$i_T = i_f + i_c \tag{14}$$

From (12) and (13)

$$i_T = \frac{4.022}{\eta^{2/3}} \times 10^5 D^{\frac{1}{2}} c^o m^{2/3} t^{1/6} + C\Delta E \frac{4.836}{\eta^{2/3}} m^{2/3} t^{-1/3} \tag{15}$$

From this expression we can determine the point of minimum current in the drop life when $di/dt = 0$. Therefore from (15)

$$t^{\frac{1}{2}}_{min} = \frac{C\Delta E}{D^{\frac{1}{2}} c^o} \times 2.404 \times 10^{-5} \tag{16}$$

Equation (16) predicts that the current will pass through a minimum during the lifetime of a drop if reversible ion transfer occurs. We will attempt to evaluate the surface concentration required to obtain the results shown in Fig.(2.5) and compare this value with the value obtained from thermodynamic predictions.

The species being transferred, as previously suggested, is likely to be Na^+ since the transfer potential of TPB^- ($\psi^o_{TPB} = 0.364$) is more negative than that of Na^+. The latter quantity has been measured by Abraham et al, 24.7 kJ mol^{-1} or 46.8 kJ mol^{-1} and also calculated at 31.0 kJ mol^{-1} (72,73). The averaged value appears to be too low when compared with the values of transfer potentials of K^+, Rb^+ and Cs^+ (25.6 kJ mol^{-1}, 24.7 kJ mol^{-1} and 23.8 kJ mol^{-1} (72) respectively.

A value of D_{Na^+} was calculated from the known diffusion coefficient for Cs^+ in dichloroethane ($D_{Cs^+} = 1.3 \times 10^{-5}$ $cm^2 s^{-1}$)
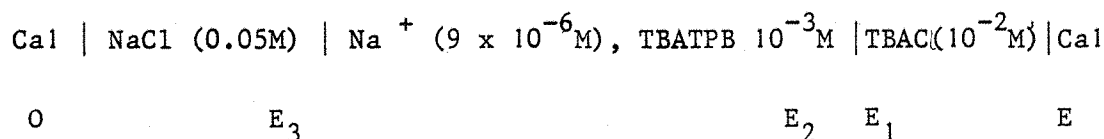
(74) and considering that this quantity is inversely proportional

to the ionic radius

$$D_i r_i = \frac{kT}{6\pi\eta} \qquad (17)$$

where η = viscosity (75). A value of $D_{Na^+} = 2.2 \times 10^{-5}$ $cm^2 s^{-1}$

is obtained.

The potential of zero charge from this system has been

measured and is equal to -0.300V (76) and from the results of

Fig.(2.5) a surface concentration of $C^o = 9 \times 10^{-6}M$ can be

calculated assuming a diffusionally controlled process.

This surface concentration must be compared with the potential

of the cell:

$$Cal \mid NaCl\ (0.05M) \mid Na^+\ (9 \times 10^{-6}M),\ TBATPB\ 10^{-3}M \mid TBAC(10^{-2}M) \mid Cal$$

$$0 \qquad\qquad E_3 \qquad\qquad\qquad\qquad\qquad E_2\quad E_1 \qquad\qquad E$$

The applied potential is -0.45V and is given by

$$E_{app} = (E_1 - E_2) + (E_2 - E_3) \qquad (18)$$

If the junction potentials can be disregarded,

$$E_1 - E_2 = -\psi^o_{TBA^+} - \frac{RT}{F} \ln \frac{a^w_{TBA^+}}{a^o_{TBA^+}} \qquad (19)$$

$$E_2 - E_3 = \psi^o_{Na^+} + \frac{RT}{F} \ln \frac{a^w_{Na^+}}{a^o_{Na^+}} \qquad (20)$$

The standard potential of TBA^+ is $\psi^o_{TBA} = -0.226V$ (56). In order

to calculate the activity of TBA^+ in the oil phase, we shall

assume $\gamma_+ = \gamma_- = \gamma_{\pm}$ and use the extended Debye-Hückel theory.

$$\log \gamma_{\pm} = \frac{-A\sqrt{C(1-\alpha)}}{1 + aB\sqrt{C(1-\alpha)}} \qquad (21)$$

where α is the degree of association of TBATPB and A and B are constants of the theory. a is the sum of the ionic radii and taken equal to 6.8 $\overset{o}{A}$. The association constant is given by

$$K_{assoc} = \frac{\alpha\gamma_{TBATPB}}{(1-\alpha)^2\gamma^2 C} \qquad (22)$$

and from (21) and (22) a value of $\gamma_{\pm} = 0.518$ was calculated for the $10^{-3}M$ TBATPB solution. Replacing into (19) and (20), a value of $\psi^o_{Na+} = 0.358V$ can be calculated using $C^o_{Na+} = 9 \times 10^{-6}M$. This value is within the expected range of values previously discussed and indicates that the ionic transfer implied in the results of Fig.(2.5) is in agreement with thermodynamic data.

Fig.(2.6) shows the instantaneous I-t curves and Fig.(2.7) their log I-log t analysis for TEA^+ transfer. The latter gives a linear relationship except towards the end of the drop lifetime, of gradients 0.16 and 0.19. The Ilkovic equation predicts a gradient of 0.167 for a diffusion controlled process (71).

The logarithmic analysis of the polarograpic wave (Fig.2.8) from the relation (71):

$$\Delta^o_w \psi = -\Delta G^{o \, o \to w}_{t \, i} /ziF + RT/2ziF) \ln D_{i(w)}/D_{i(w)} +$$

$$RT/zF \ln \frac{<Id> - <I>}{<I>} \qquad (23)$$

where D = diffusion coefficient, ΔG_{tr} = Gibbs energy of transfer,

a slope of 70 mV is obtained. Although this value is higher than the expected 60 mV it still tends to confirm that the process of TEA$^+$ transfer is reversible and diffusion controlled.

The Ilkovic equation (71):

$$< I_{LIM} > = \frac{4.022 \times 10^5}{d_w^{2/3}} z D^{\frac{1}{2}} C_m^{*2/3} t_{max}^{1/6} \qquad (24)$$

where $C^* $ = bulk concentration (mole.cm^3), m = flow rate (mgs^{-1}) and D = diffusion coefficient (cm^{2}s^{-1}) can also be used to calculate the diffusion coefficient of TEA$^+$. In the example shown in Fig.(2.3) z = 1, $< I_{LIM} >$ = 2.6 x 10^{-6} A, C^* = 60 x 10^{-9} mol.cm^{-3}, m = 9.87 mg/s and t_{max} = 3.0s, therefore a diffusion coefficient $D^o_{TEA^+}$ = 4.5 x 10^{-6} cm^{2}s^{-1} can be calculated. A value of $D^W_{TEA^+}$ can be estimated considering that the diffusion coefficient is inversely proportional to the viscosity (eqn.17)

$$\frac{D_1}{D_2} = \frac{\eta_2}{\eta_1} \qquad (25)$$

Taking η_{DCE} = 0.00871 and η_w = 0.01002 a value of $D^W_{TEA^+}$ = 5.2 x 10^{-6} cm^{2}s^{-1} is obtained. From the above results, E$^{\ominus}$ = -275 mV is obtained and from:

$$E^{\ominus} = \Delta^W_o \psi^o_{TEA^+} - \Delta^W_o \psi^o_{TBA^+}$$

where $\Delta^W_o \psi_{TBA^+}$ = -0.226V (56), the transfer potential calculated is:

$$\Delta^W_o \psi_{TEA^+} = 0.048V$$

This polarographic value is in good agreement with previously reported values (0.049V (72)).

From the above analysis it can be concluded that the technique of polarography using EDE can be analysed in an analogous manner to a DME. The results obtained for TEA $^+$ transfer are in good agreement with previously published results, although it would appear that the technique requires a little further refinement.

The determinations of drop time and flow rate, control of capacitive currents and ohmic compensation are all areas of possible improvement. Time, for the present, precluded these refinements.

2.3 PREPARATION AND CHARACTERIZATION OF AFFINITY DYES

2.3.1. Introduction

The dyes chosen were the monochlorotriazine Cibracron blue F3GA and Procion blue MX-R a dichlorotriazine. The chlorine atoms of the triazine centre are very reactive and are the point through which the dyes are most often bound to their supports in affinity chromatography. It was this point which seemed most suitable for attachment of the C_{16} hydrocarbon tail or "anchor".

2.3.2. Preparation

The Cibracron blue F3GA and the spacer arm hexadecylamine were soluble in a 3:1 v/v solution of tetrahydrofuran:water at a molar ratio of dye:spacer of 1:1.

The hexadecylamine was predissolved in tetrahydrofuran and added to an aqueous solution of 25 mM sodium hydroxide. The reaction was carried out for 18 hours at $50^{o}C$.

The tetrahydrofuran was removed under reduced pressure in a rotary evaporator and the remaining solution was centrifuged at 3000 r.p.m. for 5 minutes. The supernatant was discarded and the precipitate resuspended and again centrifuged. The remaining solid was centrifuged and dried in an oven at approximately $80^{o}C$.

The Procion blue MX-R derivative was prepared in a similar way but the reaction was completed after 5 minutes at room temperature, to give two isomers depending on which chlorine atom was replaced. Purity of products were determined via thin layer chromatography.

The bulk dye preparations were carried out by the cooperating body at CAMR.

2.2.3. Tetrabutylammonium salts of dyes

Tetrabutylammonium chloride was dissolved in water above a 1,2-dichloroethane phase and the dye (substituted) added in suspension to the aqueous phase. The mixture was stirred vigorously overnight and the dichloroethane phase, now coloured with product, filtered and washed with water three times. The concentration of product was determined from the extinction coefficient (ε) at 600 nm assuming no change in ε had occurred as a result of reaction. The tetrabutylammonium chloride was in excess.

2.3.4. Characterization of dyes

The characterization of the dyes was carried out using ultra-violet, infra-red and N.M.R. spectroscopy as well as thin layer chromatography to ascertain purity.

(i) Ultra-violet (U.V.)

The U.V. spectroscopy, Fig.(2.9) and (2.10) demonstrated that the addition of a hydrocarbon chain does not affect the λ_{max} of the dye. The chain does not cause a significant effect in the spectrum and the assumption that the extinction coefficient and λ_{max} remain the same as before modification is reasonable.

The transitions giving rise to the peaks shown in Fig.(2.9) and (2.10) for the unmodified dye are attributed to those occurring on the anthracene and attached sulphonated benzene rings and this is probably the reason why the addition of the alkyl chain to the triazine moiety does not affect λ_{max}.

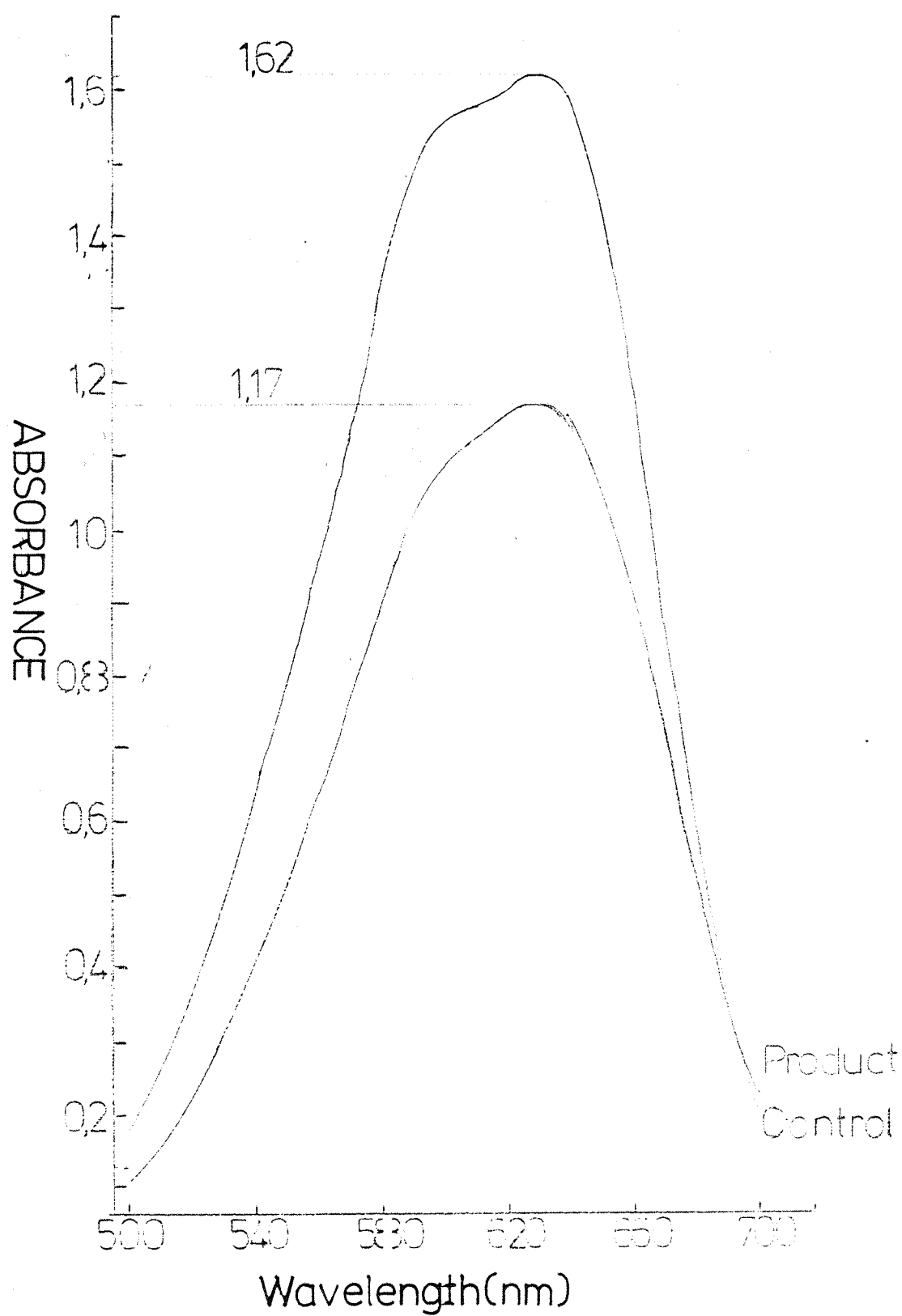The presence of the peaks indicates that the modification did not affect any of the aromatic parts of the molecules.

Figure 2.9 The ultra-violet spectrum for Cibacron blue F3GA and
Cibacron blue F3GA (C_{16}). (Conditions were THF:H_2O = 1:1V/V).
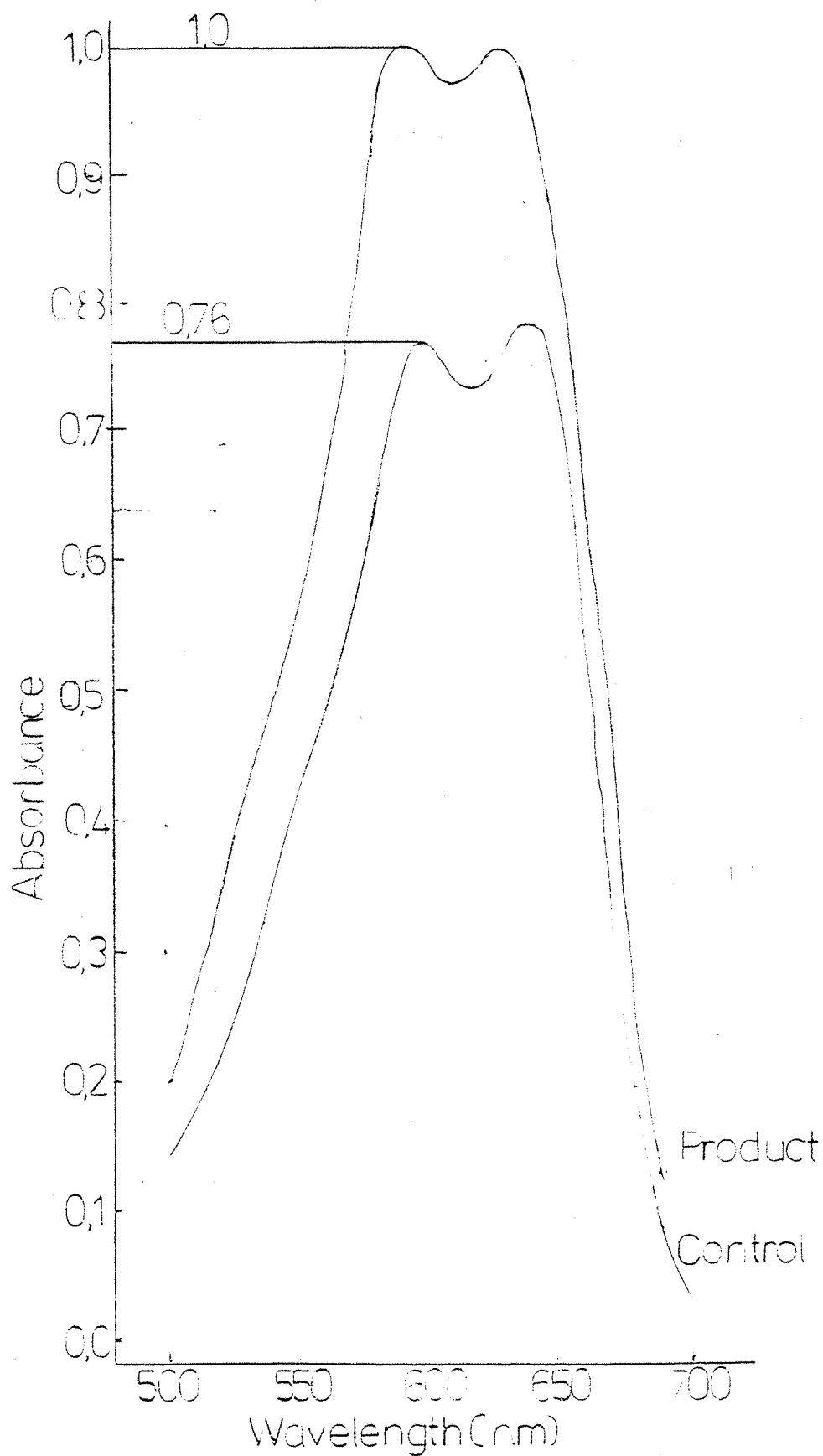
Figure 2.10 The ultra-violet spectrum for Procion blue MX-R and Procion blue MX-R(C_{16}). (Conditions were THF:H_2O = 1:1 V/V).
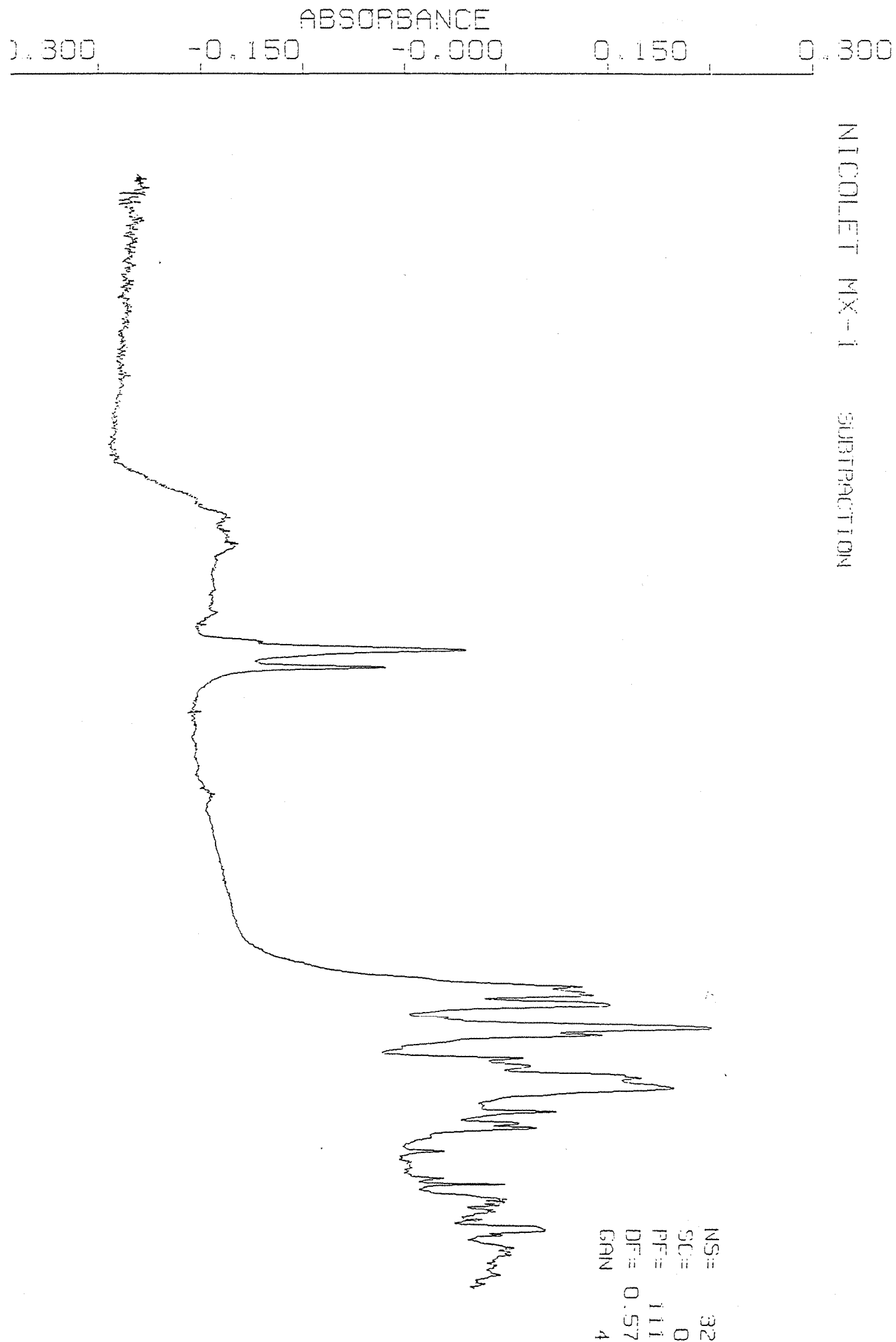
Figure 2.11a   Infra-red spectrum of Cibacron blue F3GA(C$_{16}$) as KBr disc.

Figure 2.11b   Infra-red spectrum of Cibacron blue F3GA(C_{16}) as KBr disc.
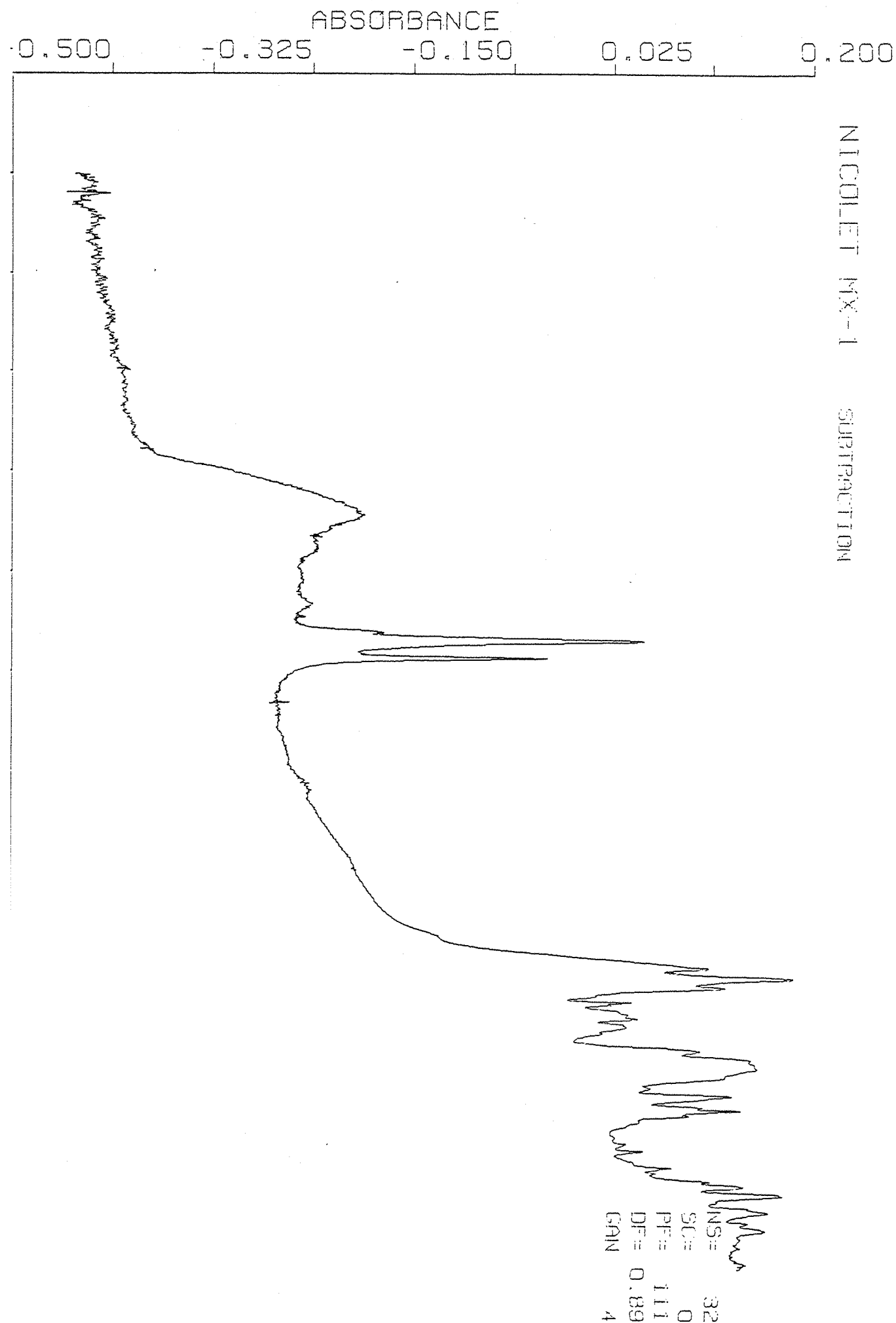Region 2000cm^{-1} – 200cm^{-1} expanded.

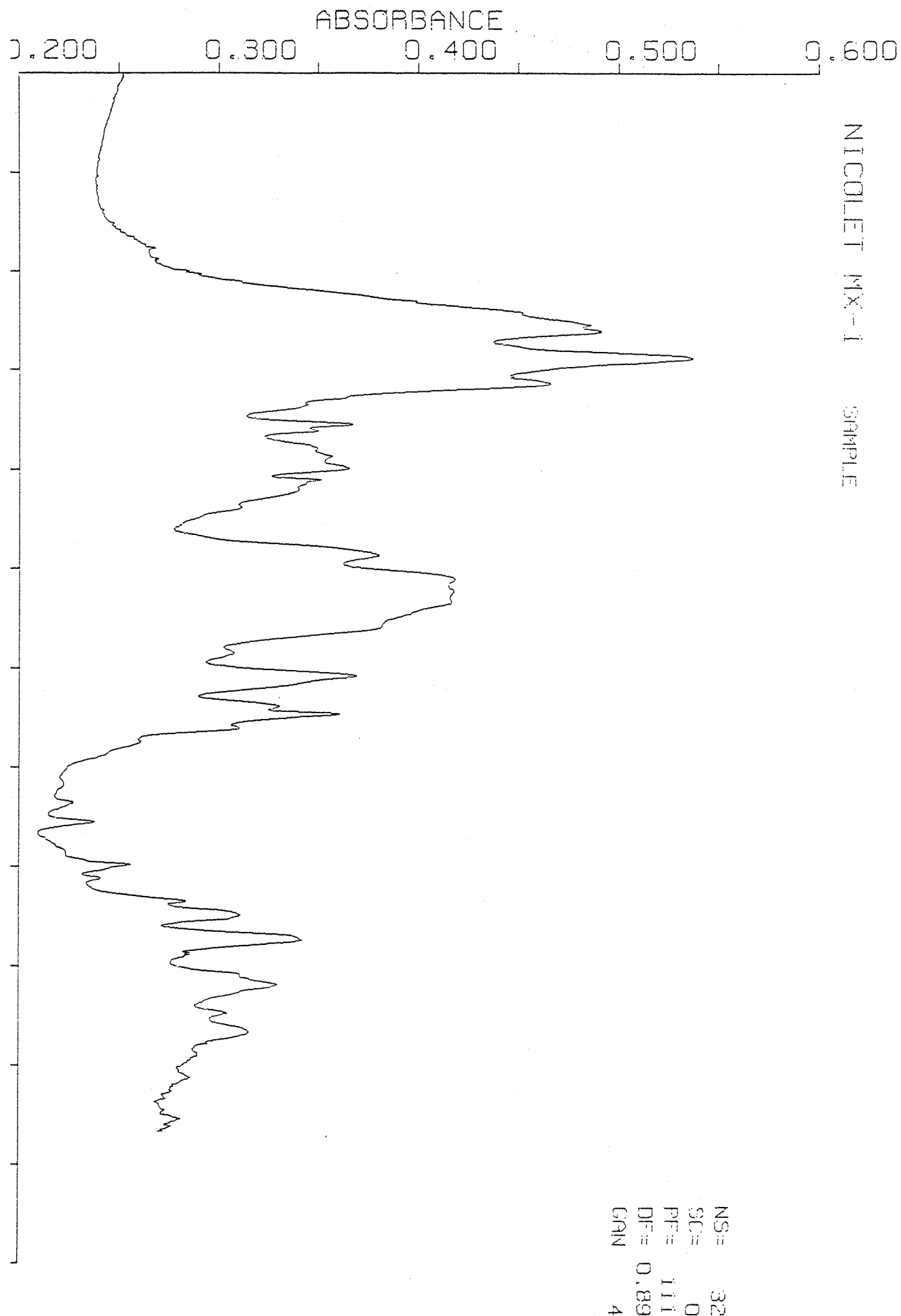Figure 2.12a   Infra-red spectrum of Procion blue MX-R(C$_{16}$) as KBr disc.

Figure 2.12b   Infra-red spectrum of Procion blue MX-R(C_{16}) as KBr disc. Region 2000-200cm^{-1} expanded.
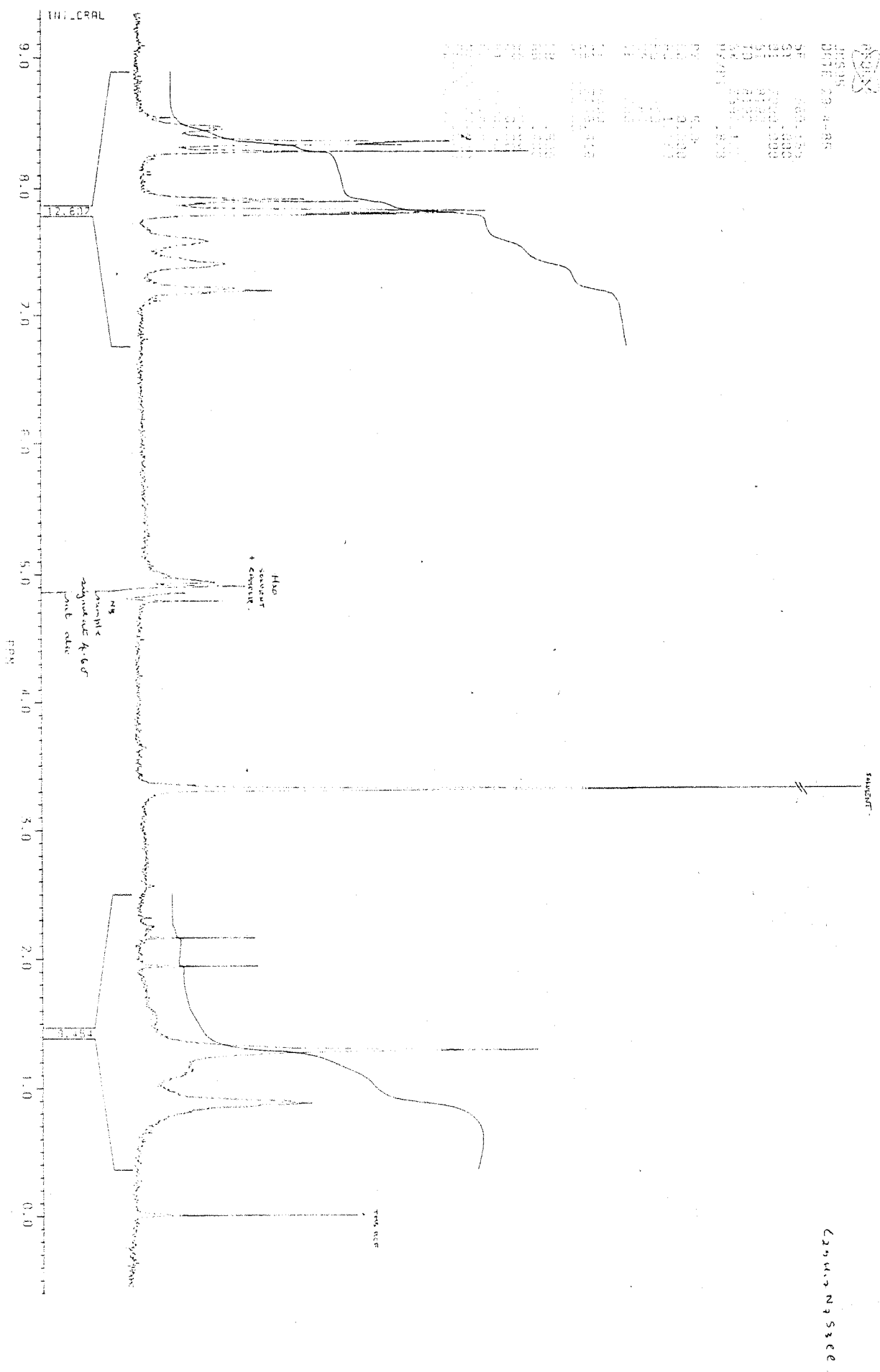
Figure 2.13 The nuclear magnetic resonance spectra (360 MHz) of Cibacron blue F3GA in deuterated methanol.
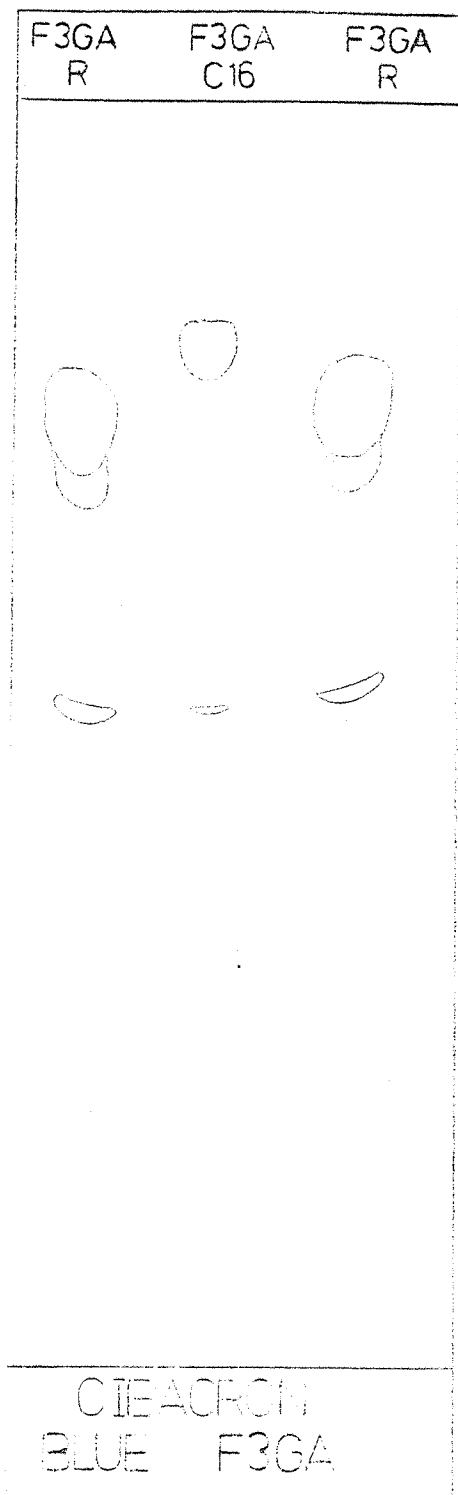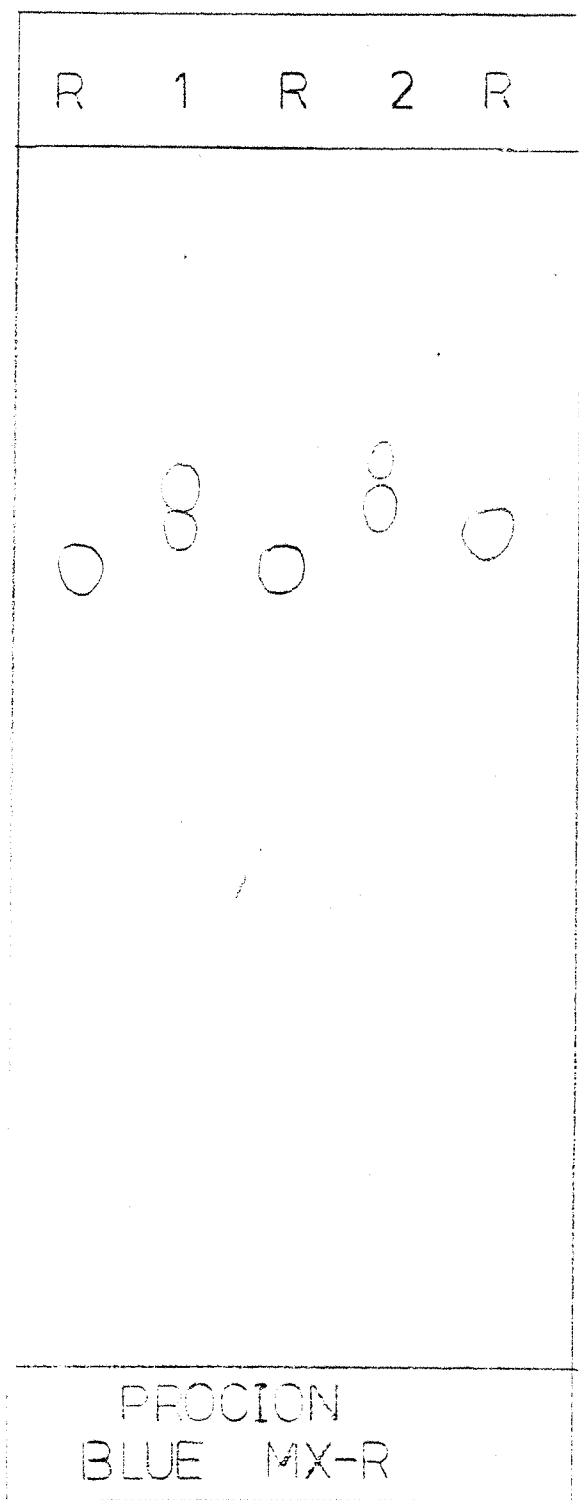
Fig 2.14

Figure 2.14   Thin layer chromatograms of the affinity dyes (THF:H_2O = 1:1V/V).

(ii) Infra-red (I.R.)

The I.R. of both dyes, Fig.(2.11) and (2.12) shows great similarity as would be expected from their predicted structures.

The spectra show the possible existence of aromatic amines and alkyl groups. The peak at around 2900 cm^{-1} is probably due to a N-H bending although also possibly associated with an aromatic C-C stretch. The peaks at 1600-800 can be assigned to both aromatic and amine characteristics, those around 1600 having the additional possibility of being the C=O bonds of the quinone.

The peaks occurring below 800 to 500 tend to suggest the presence of alkyl groups due to their absence in the I.R. of the unmodified dye (77).

(iii) Nuclear magnetic resonance (N.M.R.)

Only the N.M.R. spectra of CBA unmodified was obtained due to difficulties in obtaining a suitable solvent for the modified dyes. Fig.(2.13) demonstrates the aromaticity due to the peaks at 7.8 and 8.4 and the N-H groups at 7.2, 7.4 and 7.6. The peak at 1.2 can be tentatively assigned to the existence of N-H protons also.

(iv) Thin layer chromatography

The thin layer chromatography of CBA (Fig.2.14) demonstrates the existence of two substances as expected from the starting product being a mixture of para- and meta-substituted forms of the terminal sulphonated benzene.

The Procion blue MX-R (Fig.2.14) also shows the presence of two compounds which are also due to isomers. The presence of isomers depends on which chlorine atom of the triazine ring is replaced on the addition of the hydrocarbon chain.

The evidence obtained above coupled with the electrochemical behaviour of the dyes suggests that the dyes were modified in the manner expected.

2.4 DETERMINATION OF POTENTIAL WINDOW OF AFFINITY DYES AND

THEIR DERIVATIVES

2.4.1. Introduction

As affinity dyes have not been investigated in liquid-liquid systems previously, no information on the free energy of transfer of such dyes exists.

In such unknown systems it is convenient to carry out first orientation experiments in which the interfacial potential is determined by the partition of a potential determining ion and the dye concentration in equilibrium in both phases determined spectrophotometrically. The pH can also be varied to ascertain its effect on the free energy of transfer.

2.4.2. Theory

By putting an ion such as TPB$^-$ in the aqueous phase we have an anion which will partition into dichloroethane. If the free energy of transfer of the dye (in the organic phase) is less than TPB$^-$ the anion of the dye will transfer from organic to the aqueous phase. A wider range of potentials can be investigated by the use of TBACl in the aqueous phase which makes the potential more positive.

Also, the potential can be altered by changing the concentrations of the partitioning ion in each phase.

$$\bar{\mu}^{org}_{TPB^-} = \bar{\mu}^{w}_{TPB^-} \tag{26}$$

$$\text{and} \quad \bar{\mu}^{org}_{TPB^-} = \mu^o_{TPB^-} + RT \ln a^{org}_{TPB^-} - zF\,\psi^{org}_{TPB^-} \tag{27}$$

$$\bar{\mu}^{w}_{TPB^-} = \mu^o_{TPB} + RT \ln a^{w}_{TPB^-} - zF\,\psi^{w}_{TPB^-} \tag{28}$$

The interfacial potential difference is given by:-

$$\Delta^w_o \psi_{TPB^-} = \psi^w - \psi^o = \psi^o + \frac{RT}{F} \ln\left(\frac{a^w_{TPB^-}}{a^o_{TPB^-}}\right) \tag{28a}$$

and in the case of TBA $^+$ partition:

$$\Delta^w_o \psi_{TBA^+} = \psi^w - \psi^o = \psi^o_{TBA^+} + \frac{RT}{F} \ln \frac{a^o_{TBA^+}}{a^w_{TBA^+}} \quad (29)$$

Hence if we consider equation (28), if $a^{org}_{TPB^-}$ is increased the potential difference will decrease by 60 mV for a 10 fold difference in activity and increase by 60 mV if $a^{org}_{TPB^-}$ is decreased.

Although the free energy of Na $^+$ is close to that of TPB $^-$ its effect can be disregarded as a first approximation as the Na $^+$ concentration is negligible in the organic phase. PO_4^{2-} will probably be too well solvated to transfer within the potential window and Cl $^-$ will have no effect since their free energy of transfer is much greater than TBA $^+$. Therefore, an estimate of the standard potential or transfer of the dyes can be obtained spectrophotometrically by studying the dye partition for different potential determining ions at different concentrations.

2.4.3. Experimental

The 1,2-dichloroethane phases were made up of 10^{-2}M or 10^{-3}M solution of tetrabutylammonium tetraphenylborate as well as a 70 µM solution of the respective tetrabutylammonium salt of the dye, substituted and unsubstituted.

The aqueous phases were made up of 10^{-2}M sodium hydrogen phosphate buffer for pH values of 6.0, 7.0 and 8.0 and also of 10^{-2}M or 10^{-3}M sodium tetraphenylborate or tetrabutylammonium chloride. The concentration of the common partition ion was varied in order to

find the effective potential window. The flasks containing the aqueous and organic phases were shaken vigorously and allowed to settle overnight. The concentration of dye left in the dichloro-ethane phase was determined using a U.V. spectrometer.

The effect of altering the pH to 1 and 14 was also determined.

2.4.4. Results

The results show (Tables 2.1, 2.2, 2.3) that for all pH's considered the dyes will be transferred across the interface at potentials more negative than -0.305V and will remain in the organic phase at potentials more positive than 0.167V, thereby implying that the transfer potential for both dyes lies within the region of potential 0.167V to -0.305V which is in agreement with the surface tension results (vide infra). The concentration of modified dye in the aqueous phase could not be determined because of the appearance of a collapsed monolayer in the aqueous phase and as no dye remained in the organic phase the concentration remaining here could not be determined either.

When TBACl was added in excess to the aqueous phase the dye was pushed back into the organic phase and TBATPB precipitated in the aqueous phase.

In conclusion, it was seen that the transfer potential of the dye occurred within the polarization window determined by the base electrolyte TBATPB and therefore this system could be used to investigate the affinity dyes further by electrochemical techniques.

Table 2.1. CBA F3GA $(C_{16}NH_2)TBA_3$

	pH	Concentration A_Q (molar) Org.	Description of Phases	$\Delta_w^o \psi$ (v)
1		$10^{-2} - 10^{-2}$	Organic Clear Aqueous L/Blue PPT	−0.364
2	6.0	$10^{-3} - 10^{-2}$	Clear " L/Blue PPT	−0.423
3		$10^{-3} - 10^{-3}$	Clear " L/Blue PPT	−0.364
3		$10^{-2} - 10^{-3}$	Clear " L/Blue PPT	−0.305
5		$10^{-2} - 10^{-2}$	Organic Clear Aqueous L/Blue PPT	−0.364
6	7.0	$10^{-3} - 10^{-2}$	Clear " L/Blue PPT	−0.423
7		$10^{-3} - 10^{-3}$	Clear " L/Blue PPT	−0.364
8		$10^{-2} - 10^{-3}$	Clear " L/Blue PPT	−0.305
9		$10^{-2} - 10^{-2}$	Organic Clear Aqueous L/Blue PPT	−0.364
10		$10^{-3} - 10^{-2}$	Clear L/Blue PPT	−0.423
11	8.0	$10^{-3} - 10^{-3}$	Clear L/Blue PPT	−0.364
12		$10^{-2} - 10^{-3}$	Clear L/Blue PPT	−0.305

Table 2.2.   CBA F3GA TBA$_3$

	pH	Concentration (molar) AQ. | ORG.	Description of Phases		$\Delta_w^o \psi_{(v)}$
1		$10^{-2} - 10^{-2}$	Organic Clear	Aqueous Deep Blue	−0.364
2		$10^{-3} - 10^{-2}$	Clear	Deep Blue	−0.423
3	6.0	$10^{-3} - 10^{-3}$	Clear	Deep Blue	−0.364
4		$10^{-2} - 10^{-3}$	Clear	Deep Blue	−0.305
5		$10^{-2} - 10^{-2}$	Organic Clear	Aqueous Deep Blue	−0.364
6		$10^{-3} - 10^{-2}$	Clear	Deep Blue	−0.423
7	7.0	$10^{-3} - 10^{-3}$	Clear	Deep Blue	−0.364
8		$10^{-2} - 10^{-3}$	Clear	Deep Blue	−0.305
9		$10^{-2} - 10^{-2}$	Organic Clear	Aqueous Deep Blue	−0.364
10		$10^{-3} - 10^{-2}$	Clear	Deep Blue	−0.423
11	8.0	$10^{-3} - 10^{-3}$	Clear	Deep Blue	−0.364
12		$10^{-2} - 10^{-3}$	Clear	Deep Blue	−0.305

Table 2.3.   CBA F3GA ($C_{16}NH_2$) TBA_3 with TBACl added to the aqueous phase

	pH	Concentration (molar) Aq.	Org.	Description of Phases			$\Delta_w^o\psi$ (v)
1		10^{-2}	10^{-2}	Organic Deep Blue	Aqueous Clear		+0.226
2	6	10^{-3}	10^{-2}	Deep Blue		Clear	+0.167
3		10^{-3}	10^{-3}	Deep Blue		Clear	+0.226
4		10^{-2}	10^{-3}	Deep Blue		Clear	+0.285
5		10^{-2}	10^{-2}	Organic Deep Blue	Aqueous Clear		+0.226
6	7	10^{-3}	10^{-2}	Deep Blue		Clear	+0.167
7		10^{-3}	10^{-3}	Deep Blue		Clear	+0.226
8		10^{-2}	10^{-3}	Deep Blue		Clear	+0.285
9		10^{-2}	10^{-2}	Organic Deep Blue	Aqueous Clear		−0.226
10	8	10^{-3}	10^{-2}	Deep Blue		Clear	−0.167
11		10^{-3}	10^{-3}	Deep Blue		Clear	−0.226
12		10^{-2}	10^{-3}	Deep Blue		Clear	−0.285

At the pH's similar behaviour to that described above occurred. Also

similar results occurred with Procion-blue MX-R.

2.5 CYCLIC VOLTAMMETRY

2.5.1. Experimental

The cell used for cyclic voltammetry is shown in Fig.2.15. A flat interface of 0.8 cm^2 was used due to the large variations of interfacial tension which occurs as the potential is swept. This effect makes the use of a hanging drop electrode difficult.

The base electrolytes used were $10^{-3}M$ TBATPB in Analar 1,2-dichloroethane (BDH) and $10^{-3}M$ sodium hydrogen phosphate buffer pH 7.0 in triply distilled water (Na_2HPO_4 (BDH) and NaH_2PO_4 (BDH)).

The cell was thermostatted at $25^oC \pm 0.02^oC$. The potential was applied with a four electrode potentiostat with positive feedback for automatic ohmic potential drop compensation and a triangular waveform was applied with a Hi-Tek PPR1 waveform generator. The X-Y recorder was Bryans 2600.

2.5.2. Results

Fig.2.16 shows the cyclic voltammogram of the base electrolytes and Fig.2.17 demonstrates the effect of an addition of 10 μM CBA to the dichloroethane phase.

The characteristics of the cyclic voltammograms precluded any type of quantitative analysis but qualitatively it can be seen that there is a peak which is sweep rate dependent and will disappear at sweep rates greater than 10 mV/s. This behaviour tends to suggest an adsorption of the CBA F3GA (C_{16}) in a diffusion controlled manner. As the sweep rate is decreased the peaks approach the expected adsorption pattern as found in cyclic voltammetry of electrolyte-metal surfaces.
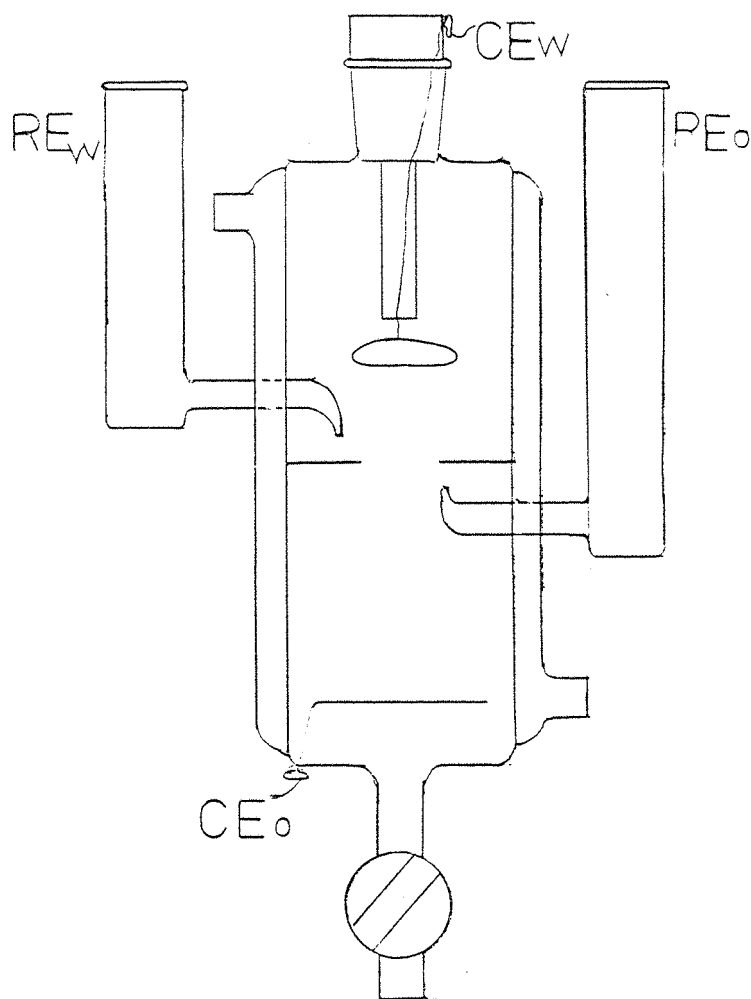
Figure 2.15   Diagram of cell used for measurement of cyclic voltammograms.
RE = reference electrode, CE = counter electrode, o = organic
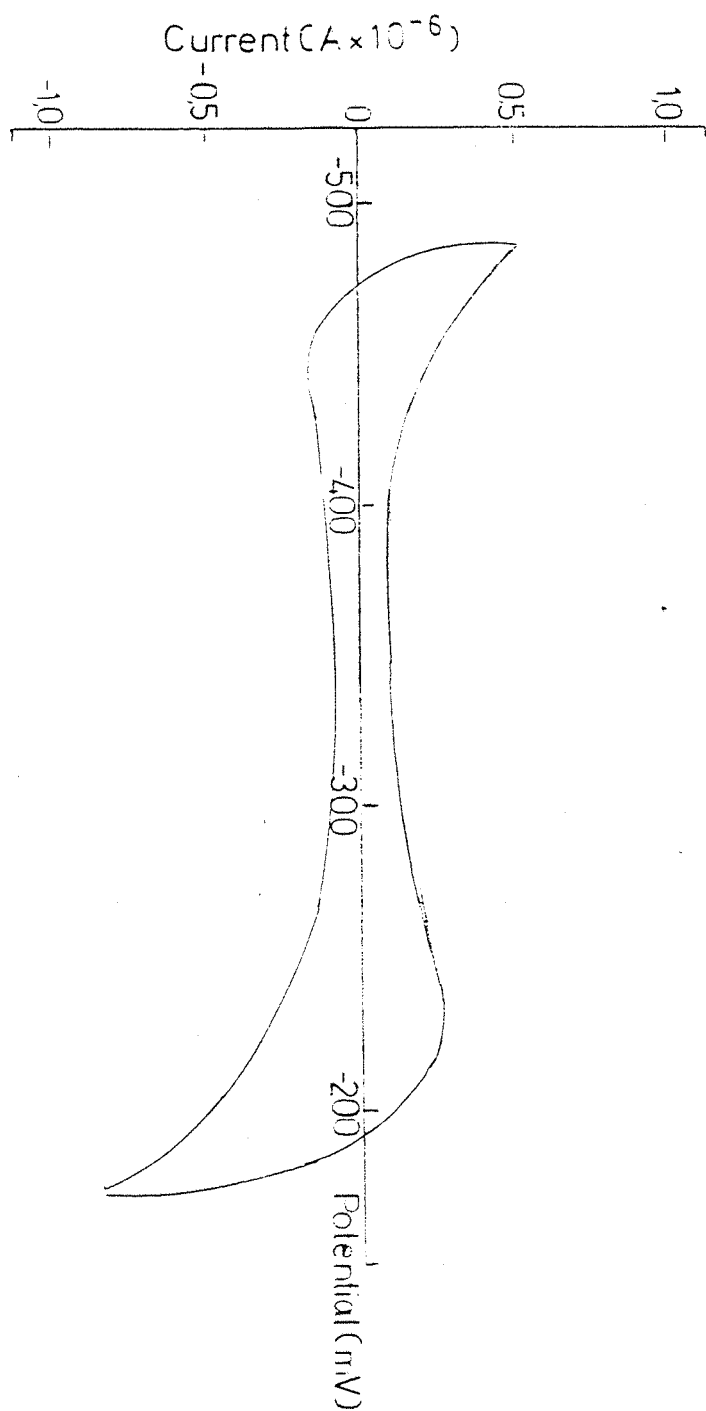w = water phases respectively.

Figure 2.16 Cyclic voltammogram of the base electrolytes; 10^{-3}M sodium hydrogen phosphate buffer pH 7.0(aq) and 10^{-3}M TBATPB (org). Area = 0.8cm².
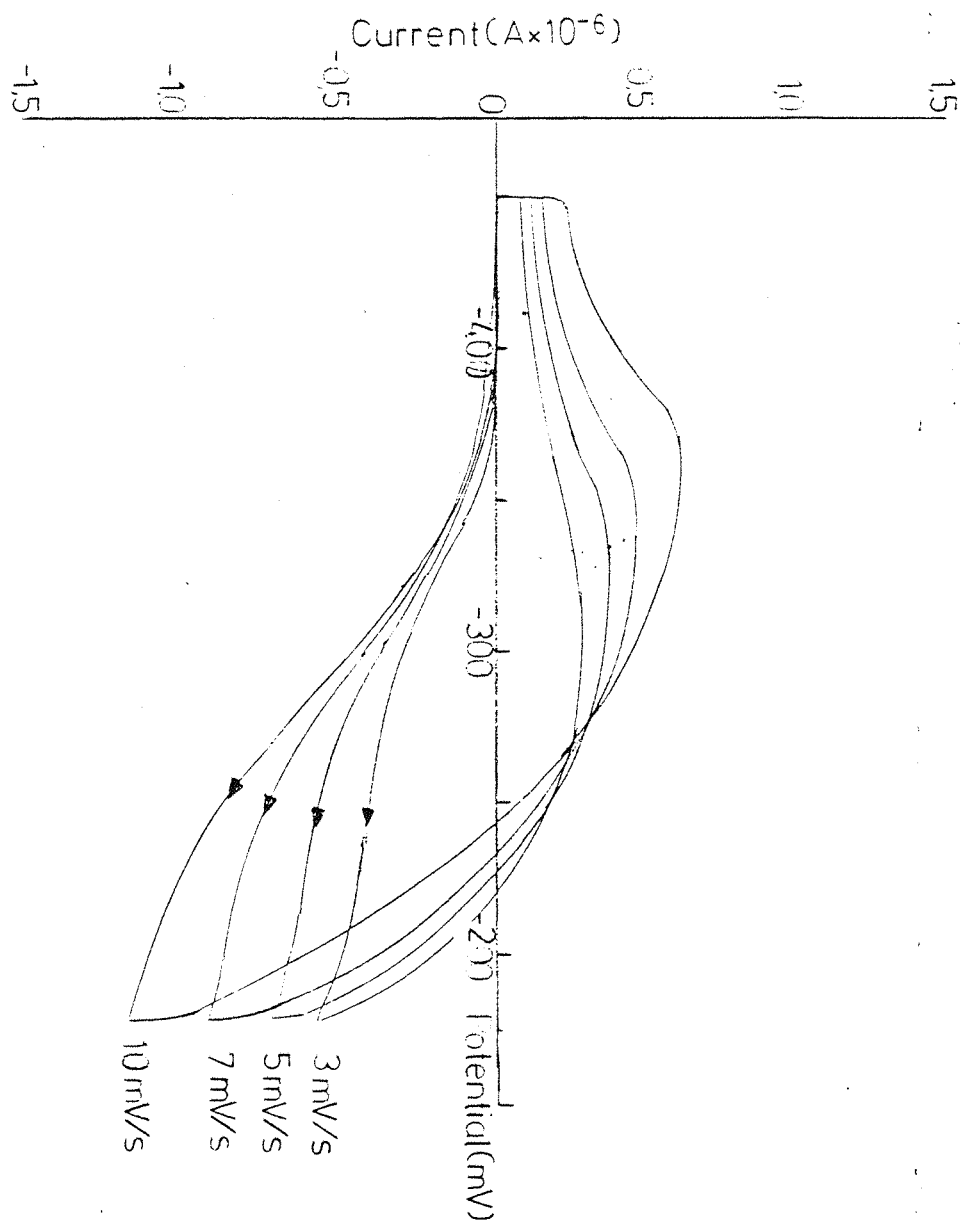
Figure 2.17   Cyclic voltammogram of 10μM Cibacron blue F3GA(C_{16}). Base electrolytes = 10^{-3}M Sodium hydrogen phasphate buffer pH 7.0(aq) and 10^{-3}M TBATPB(org).   Area = 0.8cm^2.
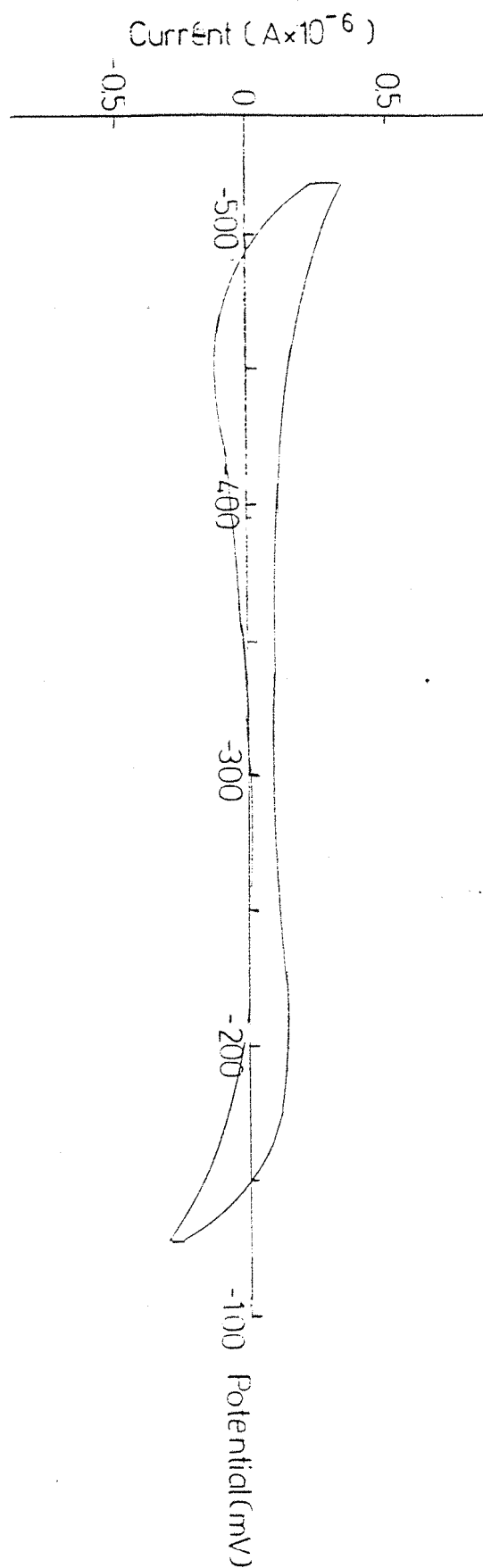
Figure 2.18   Cyclic voltammogram of 2µM Lactate dehydrogenase in water phase.
Base electrolytes = 10^{-3}M and 10^{-3}M TBATPB(org). Area = 0.4cm^2.

The origin of the charge transfer associated with these waves will be discussed in the next chapter.

Fig. 2.18 shows the effect of the protein lactate dehydrogenase on the cyclic voltammetry of the base electrolytes. The low concentration of protein, 2 μM, is not expected to be observable as a transfer. However, as the protein appears to form a skin at the interface there is a possibility of affecting the base electrolyte transfer potentials and therefore this was tested. It can be seen that this does not occur.

2.6   INTERFACIAL TENSION

2.6.1. Introduction

Interfacial tension is a contractile force which acts parallel to an interface and is a consequence of the free surface energy's tendency to diminish. It has been measured by a number of different methods which in general can be characterized into several groups.

The detachment methods are based on the force required to detach an object from an interface between two liquids e.g. Du Nouy ring, the Wilhelmy slide and the Gustalla stirrup. These methods require an enlarging and breaking up of a surface and are therefore not truly static, requiring correction factors.

Another group are based on the methods connected with the properties of a curved interface. These were originally designed for surface tension measurement e.g. capillary rise, drop weight method and maximum bubble pressure. These techniques are not absolute and require a third phase e.g. glass.

The only methods which can be considered as truly absolute rely on the geometry of a sessile or pendant drop. These techniques are developed from the work of Andreas and Hauser and are the basis of the measurements used in this study.

2.6.2. Theory

The theory is based on two equations the LaPlace equation and the local forces balance.

If a liquid surface is curved the pressure on the convex side must be less than that on the concave side by an amount dependent on the surface tension (γ).

If we consider the element below in Diagram 1.

Diag.1
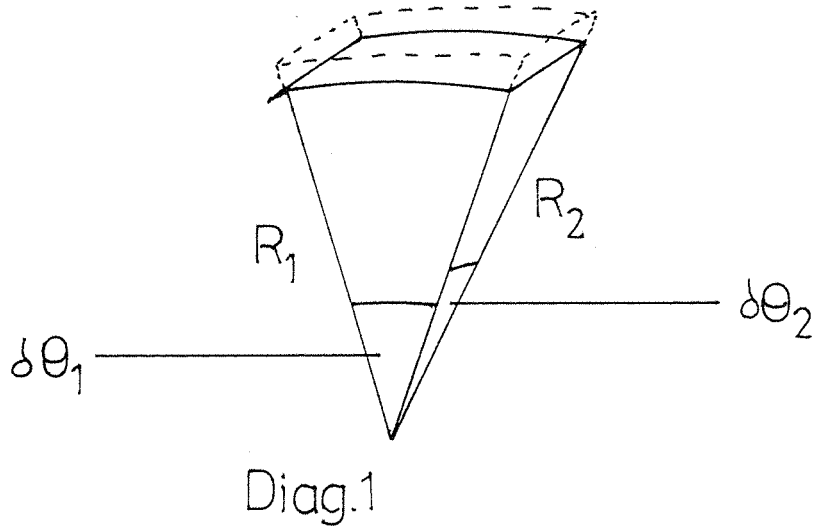
If the curved surface is moved in a manner described by the dotted line the work done in increasing the volume of the concave side must equal that to increase the area.   If the element is in equilibrium the pressure outside is P and inside is P + ∆P.

The element has an area :-

$$R_1 \delta\theta_1 R_2 \delta\theta \qquad\qquad (30)$$

where R_1 and R_2 are the principle radii of curvature of the interface. An increase of δ_r along the normal results in the performance of work given by:

$$\Delta P R_1 \delta\theta_1 R_2 \delta\theta_2 \delta_r \qquad\qquad (31)$$

This balances the increase in interfacial free energy, i.e. the product of the increase in area by the surface energy per unit area which is numerically equal to the boundary tension (γ).

After expansion the surface area is:

$$(R_1 + \delta_r) \, \delta\theta_1 (R_2 + \delta_r)\delta\theta_2 \qquad (32)$$

neglecting the term $\delta r^2 \delta\theta_1 \delta\theta_2$ this gives an area increase of

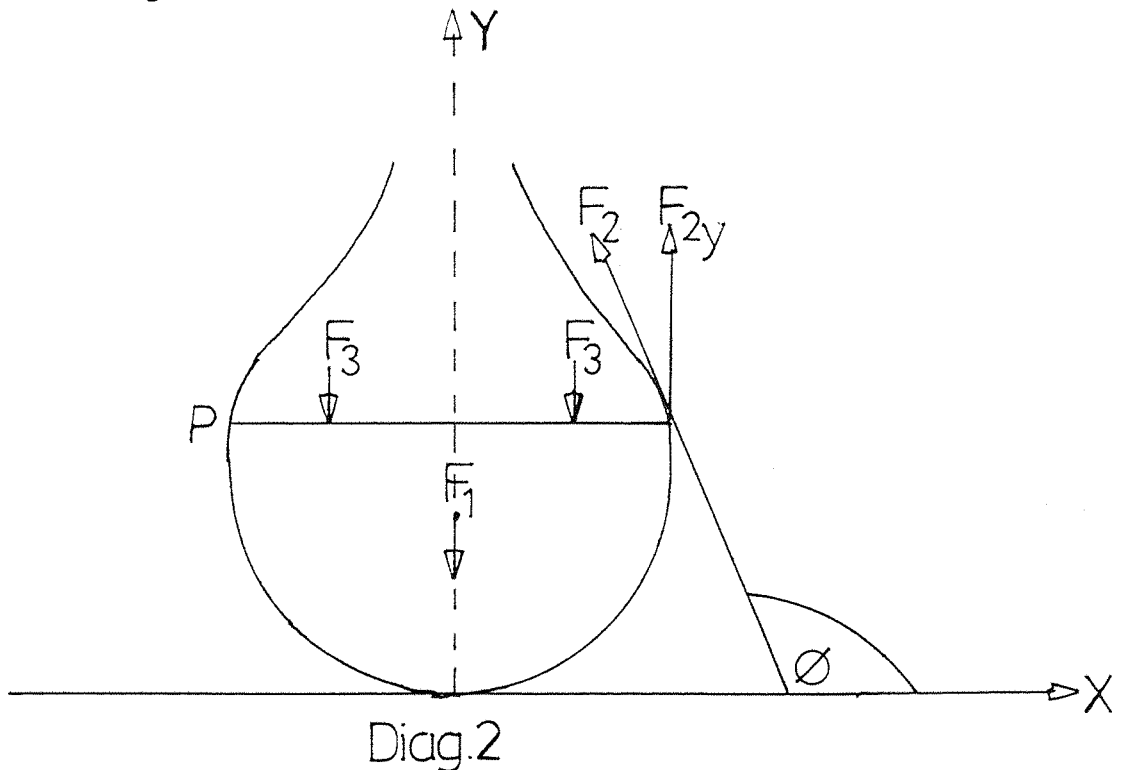$$(R_1 + R_2) \, \delta\theta_1\delta\theta_2\delta_r \qquad (33)$$

The work balance equation therefore is:

$$\Delta P R_1 R_2 \delta\theta_1 \delta\theta_2 \delta r \;=\; \gamma(R_1 + R_2)\delta\theta_1\delta\theta_2\delta r \qquad (34)$$

and therefore,

$$\Delta P \;=\; \gamma \, (1/R_1 + 1/R_2) - \text{Laplace equation} \qquad (35)$$

This equation must be applied to a pendent drop similar to that shown in Diagram 2.

Diag.2

If this drop is at mechanical equilibrium at any horizontal plane (P) all vertical forces will be balanced.   The forces acting at any plane are those shown. F_1, is the force of gravity and it equal to the weight of the liquid hanging from the plane.

Hence $F_1 = V\sigma g$ (36)

V = volume hanging under plane, σ = difference of phase densities, g = force of gravity.

F_2, is the boundary tension which acts parallel to the boundary. The vertical component $F_{2y} = 2\pi X \times \gamma \times \mathrm{Sin}\phi$ (37)

γ = boundary tension, ϕ = angle between tangent and axis, X = cross-sectional radius of plane P.

At equilibrium the forces must be balanced by the excess of pressure acting on the plane i.e. F_3.

$F_3 = \Delta P \times \pi X^2$ (38)

Now $\Delta P = \gamma \ (1/R_1 + 1/R_2)$ (35)

R_2 = internal radius of curvature

$R_2 = \dfrac{ds}{d\phi}$ (39)

R_1 = external radius of curvature

$R_2 = \dfrac{X}{\mathrm{Sin}\ \phi}$ (40)

and $F_{2y} = F_1 + F_3$ (41)

hence $2\pi X\gamma \mathrm{Sin}\phi = V\sigma g + \pi X^2\gamma \ (1/R_1 + 1/R_2)$ (42)

This equation relates the geometry of the drop to the boundary tension.

In this work the video image processor method solves this equation via the inflexion plane method as this gives a mathematically exact solution is possible. For description of experimental arrangement see (21,22). At the inflexion plane the internal radius of curvature is infinite therefore the Laplace equation becomes

$$\Delta P = \gamma / R_{infl} \tag{43}$$

where ΔP_{infl} and R_{infl} are the pressure difference and radius of curvature at the inflexion plane

therefore,
$$\gamma = \frac{V \sigma g}{2\pi X \sin\phi_{infl}} - \pi X^2 / R_1 \tag{44}$$

Now
$$R_1 = \frac{X}{\sin\phi_{infl}} \tag{45}$$

and therefore
$$\gamma = \frac{V\sigma g}{\pi X \sin\phi_{infl}} \tag{46}$$

In equations (44) to (46), X is the value of x at the inflexion plane. The method of measurement used acquires automatically the drop co-ordinates and calculates the position of the inflexion plane and V, the drop volume underneath this plane.

2.6.3 Experimental

The cell used is shown in Figure 2.19. The base electrolytes used were 10^{-3} M sodium hydrogen phosphate in triply distilled water
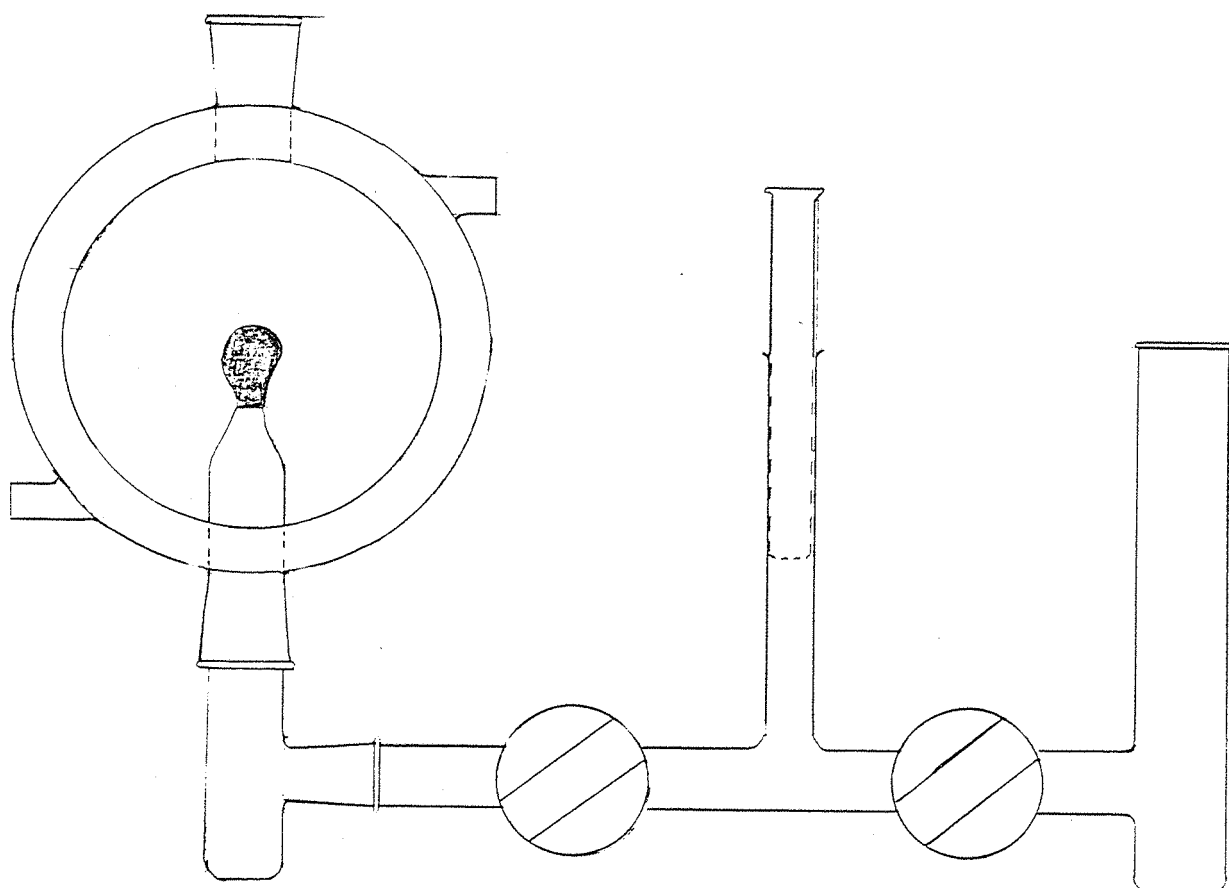
Figure 2.19   Simplified representation of the cell used for measurement
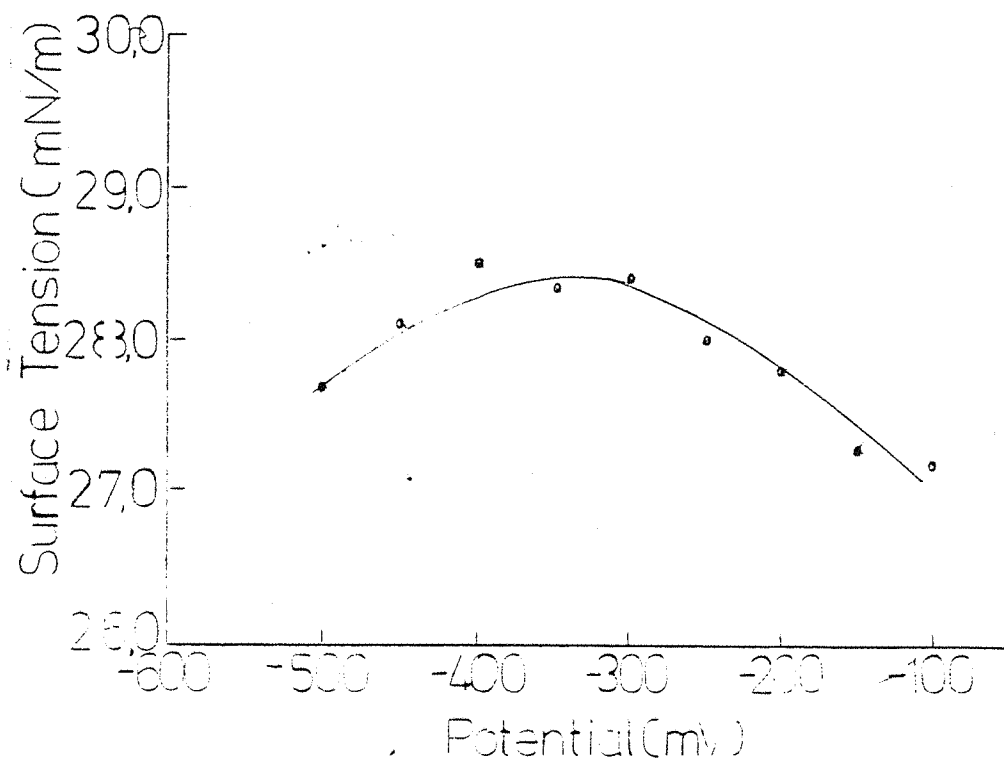of interfacial tension.

Figure 2.20 Electrocapillary curve for the base electrolyte; 10^{-3}M sodium hydrogen phosphate buffer pH 7.0(aq) and 10^{-3}M TBATPB(org).
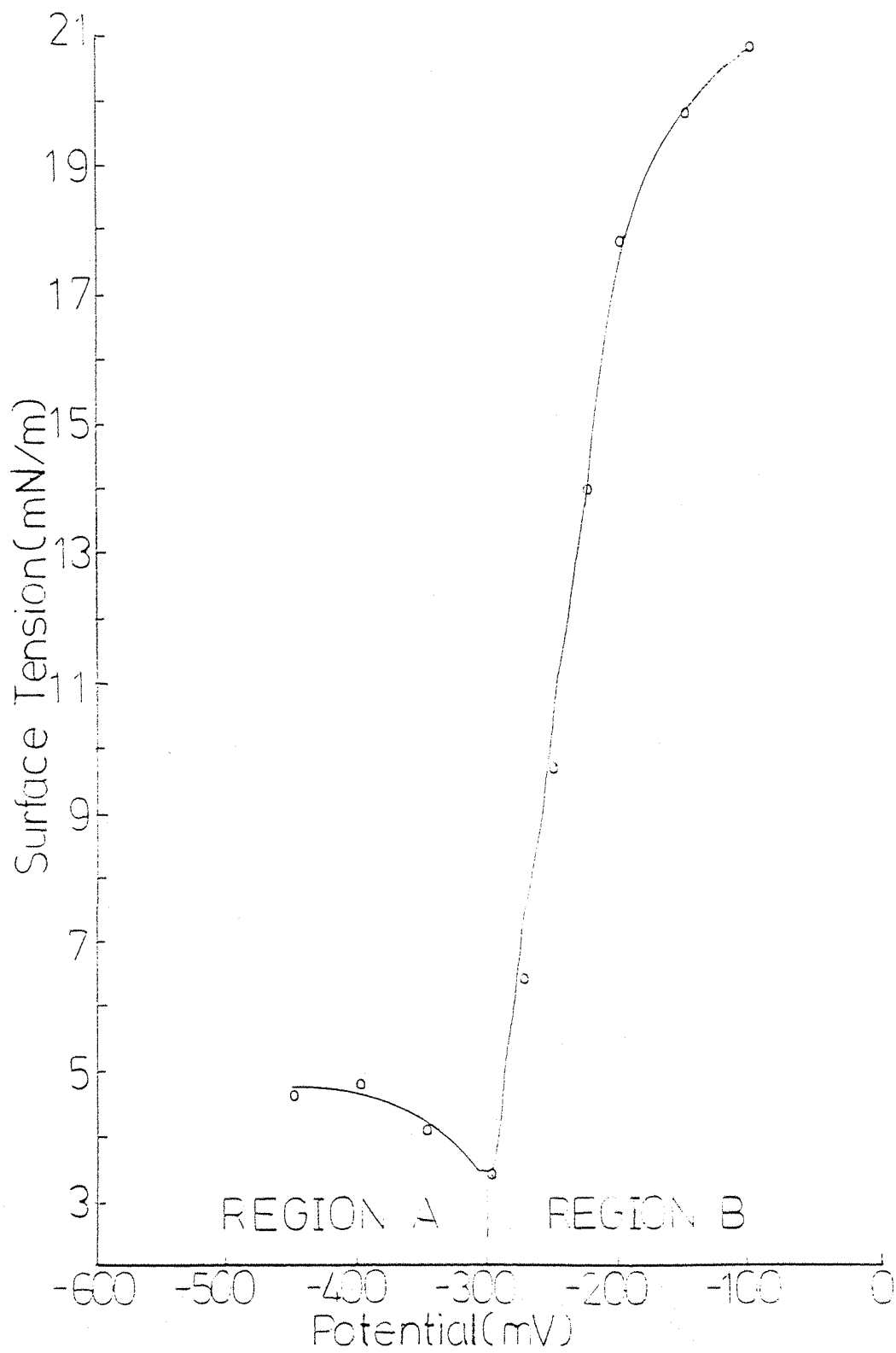
Figure 2.21 Electrocapillary curve for 20μM Cibacron blue. Base electrolyte; 10^{-3}M sodium hydrogen phosphate pH 6.0(aq) and 10^{-3}M TBATPB(org).

Figure 2.22 Electrocapillary curve for 20μM Cibacron blue. Base electrolytes; 10^{-3}M sodium hydrogen phosphate pH 7.0(aq) and 10^{-3}M TBATPB(org).

Figure 2.23   Electrocapillary curve for 20μM Cibacron blue.   Base electrolyte;
10^{-3}M sodium hydrogen phosphate pH 8.0(aq) and 10^{-3}M TBATPB(org).

Figure 2.24 Electrocapillary curve for 20μM Procion blue. Base electrolye; 10^{-3}M sodium hydrogen phosphate pH 6.0(aq) and 10^{-3}M TBATPB(org).

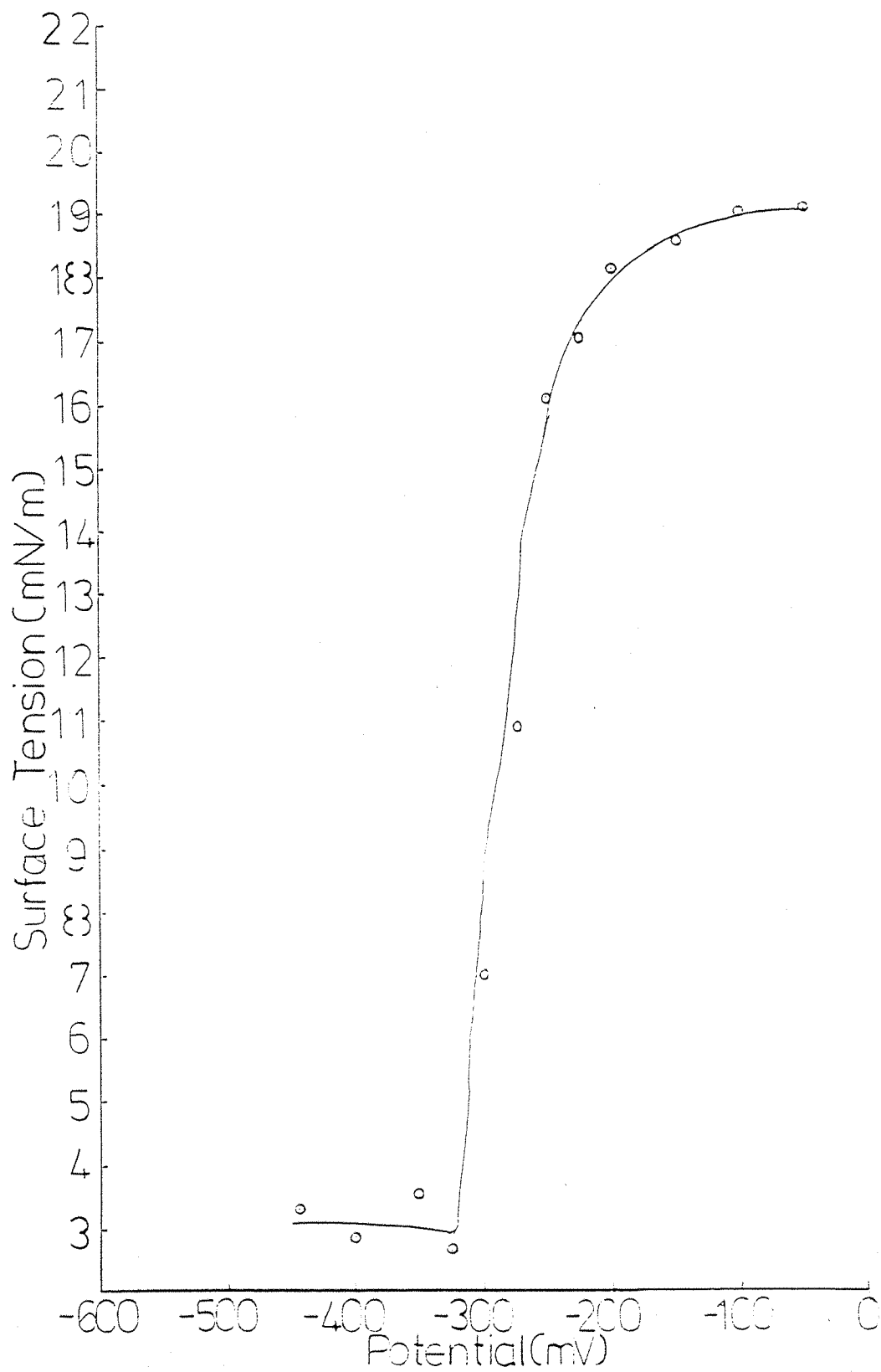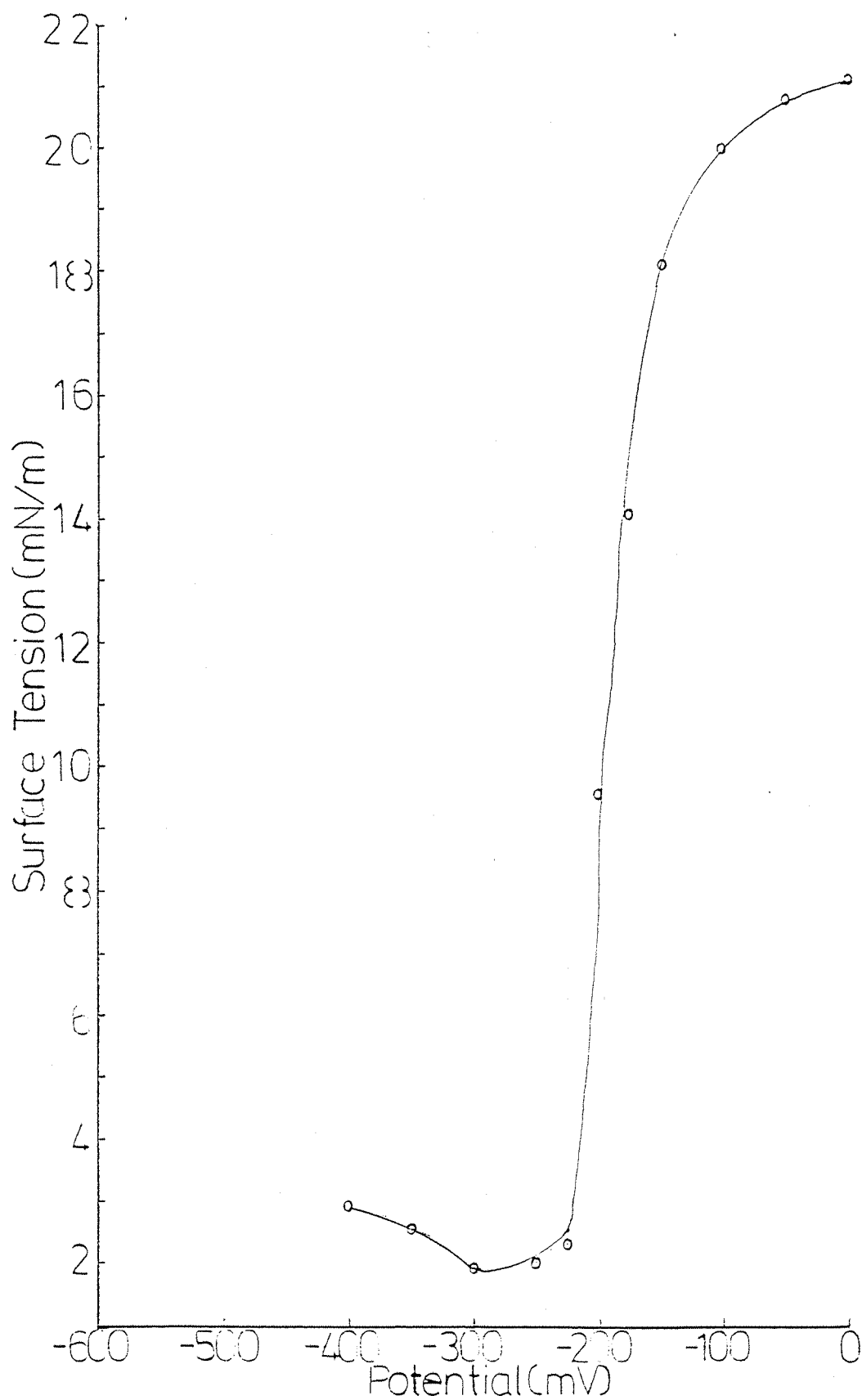Figure 2.25 Electrocapillary curve for 20μM Procion blue. Base electrolytes; 10^{-3}M sodium hydrogen phosphate pH 7.0(aq) and 10^{-3}M TBATPB(org).
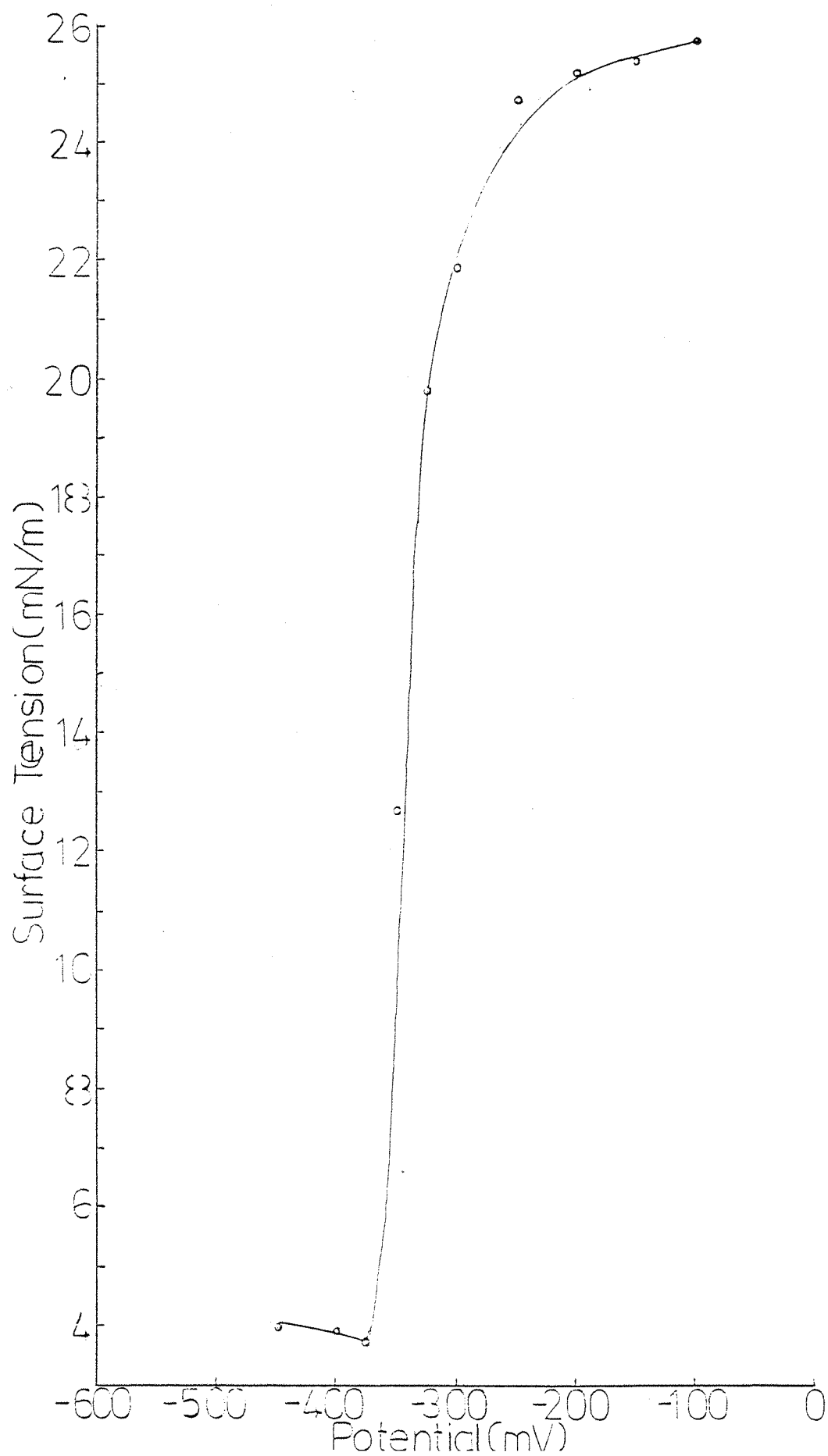
Figure 2.26 Electrocapillary curve for 20μM Procion blue. Base electrolytes; 10^{-3}M sodium hydrogen phosphate pH 8.0(aq) and 10^{-3}M TBATPB(org).
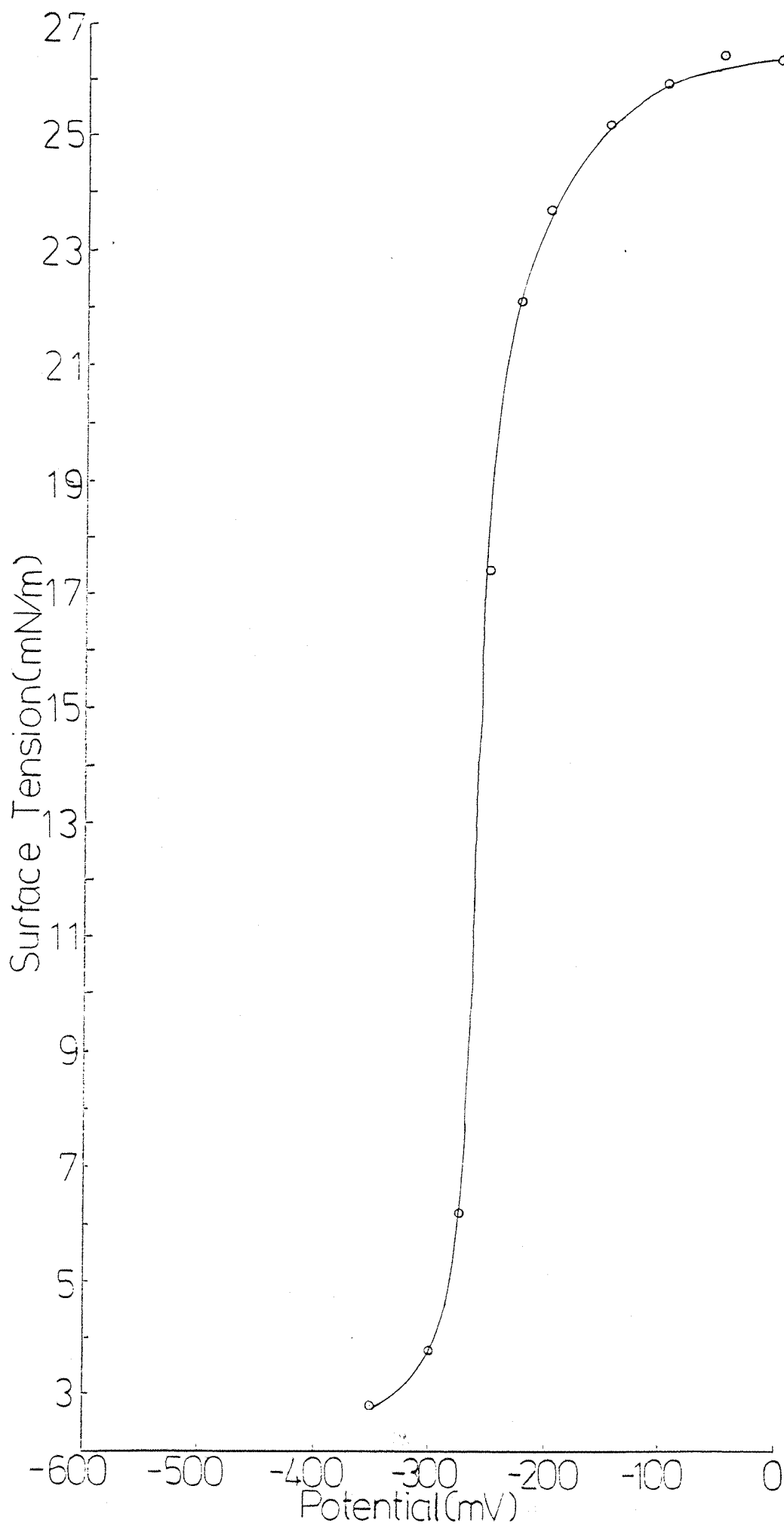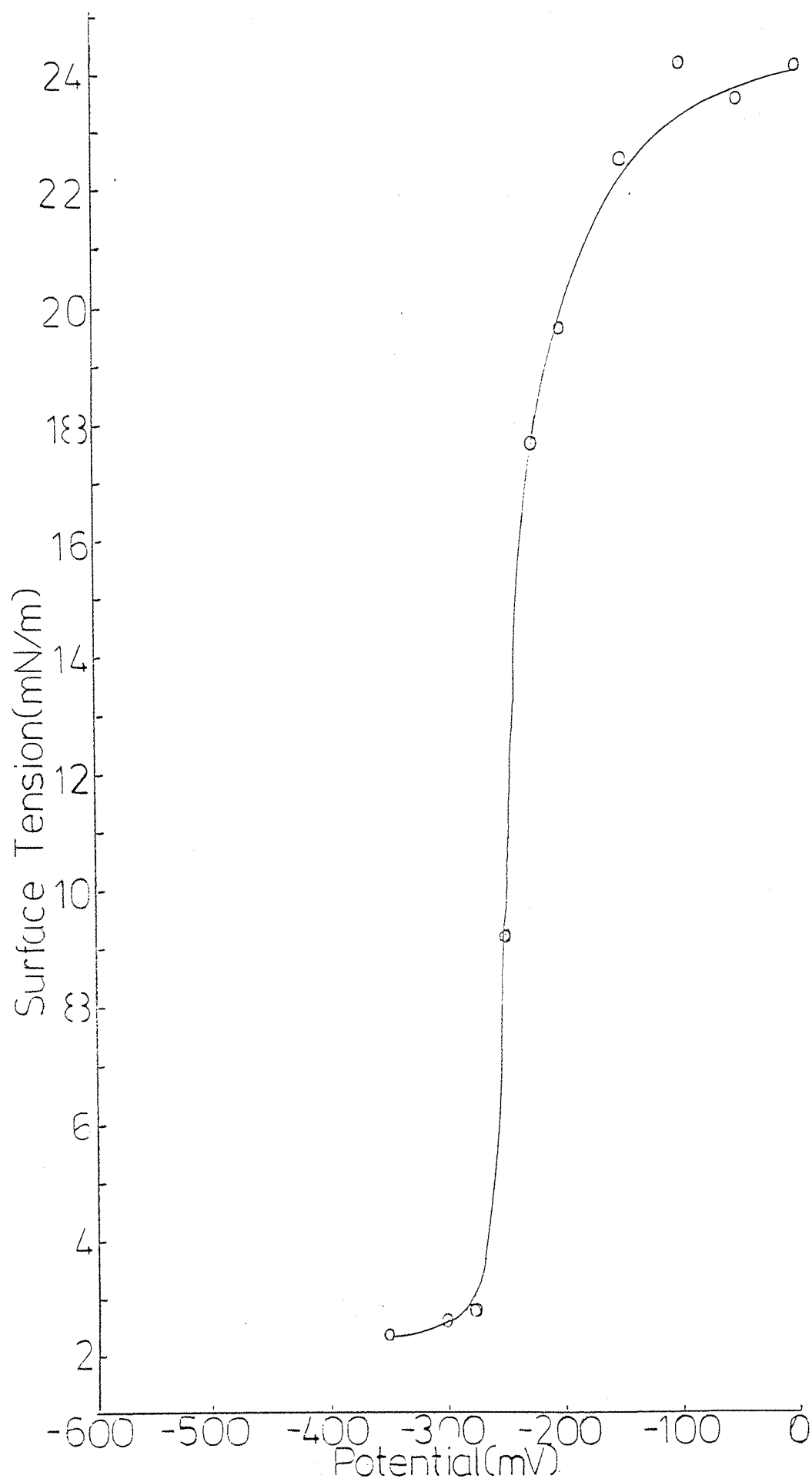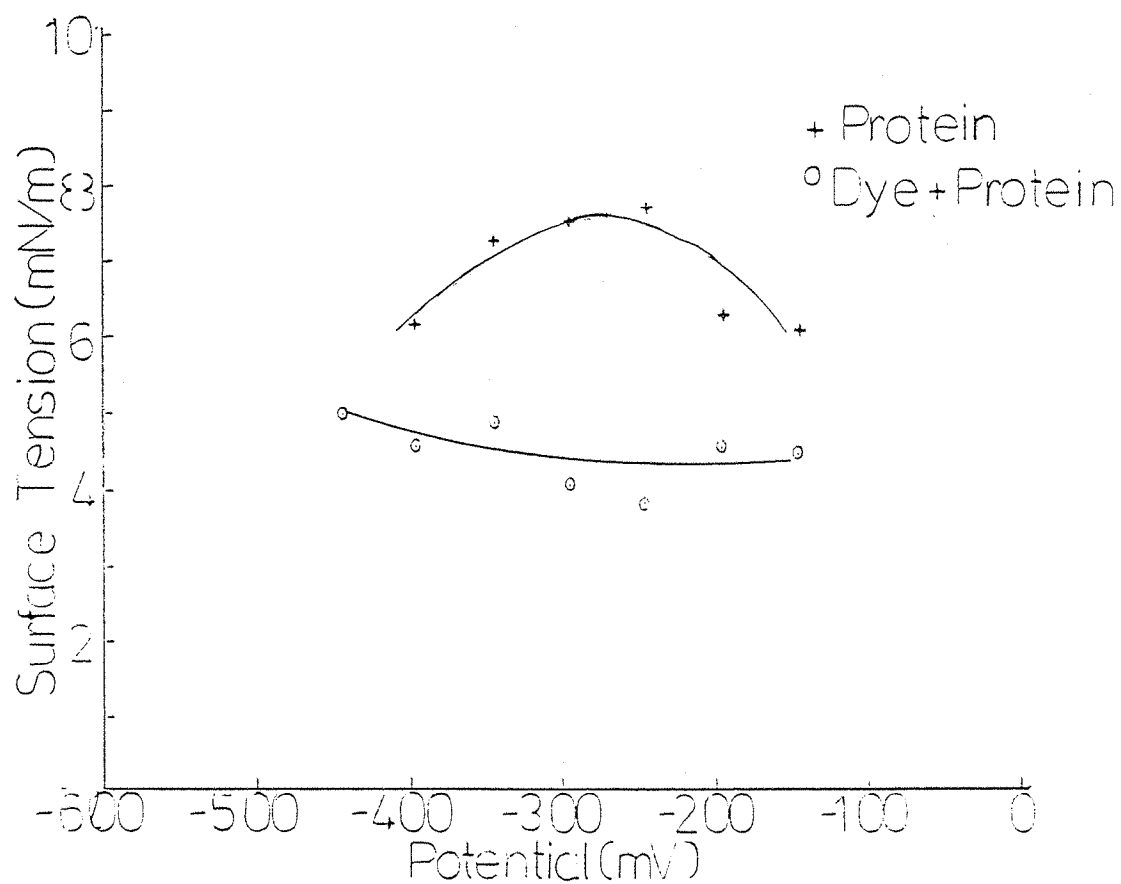
Figure 2.27 Electrocapillary curve for 2µM lactate dehydrogenase (a) in absence of dye (CBA) (+) and (b) in presence of dye (CBA) (o).

and 10^{-3} M TBATPB in Analar 1,2-dichloroethane. The cell was
thermostated at $25^{\circ}C \pm 0.02^{\circ}C$ and the potential adjusted via a
four electrode potentiostat with positive feedback.

The surface tension was measured using the inflexion plane
technique with a video image profile digitzer (21) (22). The
computer used was a DEC 11/23 and the television camera was
fitted with a Nikkon 105 mm macrolens. The protein used was
lactate dehydrogenase (2μM)(Sigma).

2.6.4. Results

Figure 2.20 shows an electrocapillary curve of the base
electrolytes used and Figures 2.21 - 2.26 demonstrate the effect
of the addition of 20μM of either Cibracron blue F3GA (CBA) or
Procion blue MX-R to the organic phase when the bulk pH of the
aqueous phase is altered from pH 6 to 8. It can be seen that
there is a very strong potential dependence of the interfacial
tension.

Figure 2.27 demonstrates the effect on the interfacial tension
of a 2μM solution of lactate dehydrogenase buffered at pH7.0 and
also the effect of 10μM CBA added to the organic phase when lactate
dehydrogenase is present.

It can be seen that the protein has a profound effect on the
interfacial tension when CBA is not present and a skin could be
observed at the interface. The addition of CBA lowers the surface
tension even further but the skin is always present.

2.6.5 Discussion

The effect of adsorption of these dye molecules on the electrocapillary curves (Figure 2.20) is very different from the adsorption of organic molecules at a mercury-electrolyte solution interface but very closely analogous to the effect observed previously (14) with phospholipids in a similar liquid-liquid system. It is for this reason that the interpretation of the electrocapillary curves can follow a similar course. It is possible to divide the curves into two regions, A and B (Figure 2.21). Region A, at negative potentials, shows a very small change in interfacial tension with potential and Region B, at positive potentials, shows a very rapid and very significant change in interfacial tension.

If we consider the electrocapillary equation in the presence of an adsorbed neutral species, N, at an interface between water with base electrolyte $B^+ D^-$ and an organic solution containing $C^+ A^-$ (50):

$$- d\gamma = Q dE_{+(-)} + \Gamma_+^{(O,W)} d\mu_{BD} + \Gamma_-^{(O,W)} d\mu_{CA} + \Gamma_N^{(O,W)} d\mu_N \qquad (47)$$

Where Q = thermodynamic charge

$$= F (\Gamma_{C^+}^{(O,W)} - \Gamma_{A^-}^{(O,W)}) \qquad (48)$$

$\Gamma_i^{(O,W)}$ = relative surface excess concentration.

From this equation it follows that the charge in Region A is very low and suggests that an adsorbed monolayer of dye molecules has formed in this region. Region B shows a sharp increase in interfacial tension with $Q = d\gamma/dE < 0$ i.e. there is a negative charge at the interface.

The existence of a monolayer of neutral dye in Region A
Figure (2.21) is difficult to understand if the dye structure
is considered.   The sulphonic acid groups have a pka < 1 and
are therefore expected always to be in an ionized state giving
rise to a nett negative charge on the molecule.   The other
groups which can be protonated to neutralize the molecule are
the bridging NH groups and the NH_2 group of the anthracene-
sulphonic acid part of the molecule.   No data exists on the pka's
of these groups.   However, by consideration of similar compounds
(see Table 2.4) it can be concluded with resonable certainty that
the bridging NH groups will probably have a pka < 1 and are there-
fore always deprotonated and that the NH_2 group will protonate
somewhere in the range of pH under study.

It is proposed that in Region A the ionization of the CBA
molecule should be such that the sulphonic acid groups are
negative and the NH_2 group is positive (evidence for which possibly
exists from N.M.R.) giving rise to a nett negative charge of -2 per
molecule.

There are two possible ways the observed low charge on the
interface can be explained in Region A.   Either the molecule is
"pushed" up into the aqueous phase to such an extent that sheilding
of the charges in an analogous way to that described in the Debye-
Hückel theory occurs, thus neutralizing the charge, or, only a
zwitterion is formed as a consequence of the high ion pairing in
the organic phase between some of the sulphonic groups and the
TBA^+ ion.
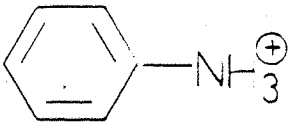
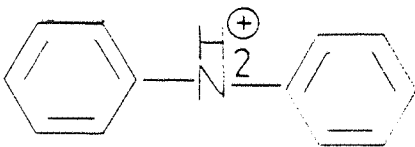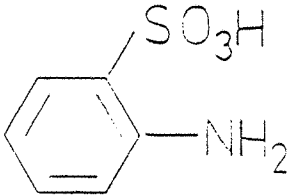| Formula	pK_a
⬡—$NH_3^{\oplus}$	4,60
H_2N—⬡—$NH_3^{\oplus}$	6,16
⬡—$\overset{\oplus}{\underset{2}{N}}H$—⬡	0,79
⬡ with SO_3H and —NH_2	3,74

TABLE 2.4   The pKa of amino groups in compounds demonstrating some resemblance to the triazine dyes used.

The first situation is highly unlikely on the grounds that
it would require a great deal of energy to lift the molecule to
such an extent that effective shielding of the charge could occur
and this hypothesis is not favoured.   Furthermore, the Debye
screening length in the concentration used is greater than the
length of the hydrophobic chain.

The second hypothesis arises from the work done with phospholipids
(14) where the Region A was explained in terms of the formation of
a zwitterion.   It is proposed that only the anthracenesulphonic
acid part of the molecule projects into the aqueous phase and
this can act as a zwitterion by virtue of the NH_3^+ and SO_3^- groups.

Region B is determined by the deprotonation of the NH_3^+ group;
as the potential becomes more positive the NH_3^+ deprotonates to
become NH_2 and the molecule acquires a nett negative charge.
This results in the dye desorbing from the interface in Region B
and an increase in interfacial tension occurs.   This rapid change
in the state of charge is in contrast to the lecithin situation
where the ionization does not appear to cause desorption in
Region B, whereas in the present case, the dye seems to be
desorbed in this region as the interfacial tension approaches the value
of the base electrolyte.   It is unexpected that only one sulphonic
acid group should be present in the aqueous phase.   However the
anthracenesulphonic acid part of the molecule is considerably more
polar, due to the NH_3^+ group and the quinone oxygens, than the
rest of the molecule and this is possibly the reason why only this
sulphonic acid group should be present in contact with the aqueous
phase.   It is proposed that the loss of polarity due to deprotonation

of the NH_3^+ group is sufficient to lead to desorption of the dye.

Evidence for this hypothesis arises from the second dye used in this study and the cyclic voltammetry. Procion blue MX-R gave similar electrocapillary curves to CBA although this dye has one less sulphonic acid group (Figure 11.). If the anthraquinone moiety zwitterion hypothesis is correct this similar behaviour would be expected since the rest of the dye molecule should have a small influence on its adsorption properties.

The cyclic voltammetry results for CBA (Figure 2.17) show the occurence of a charge transfer process in the potential range -0.35/-0.25 V. However, no net transfer of dye should occur within this potential range as shown by visual observation of the interphase. The partition experiments showed that the transfer of the dye at very negative potentials (Table 2.1) results in the formation of insoluble collapsed monolayers, an effect which could not be seen in the potential region of interest. The voltammetric peaks observed must be related to the adsorption/ desorption process previously discussed. Besides the expected increase in interfacial capacitance on desorption of the dye , deprotonation of the NH_3^+ group will also occur and the observed voltammetric waves are a result of the combination of these two effects. From the sweep rate dependence of the peak potentials, it would appear that the interfacial reaction is very irreversible and further work is necessary to understand the kinetics of adsorption-desorption.

Figure 2.27 shows the effect of 2μM lactate dehydrogenase in the aqueous phase on the interface. The protein appears to be strongly adsorbed and a skin is observed. It is believed that this skin corresponds to a layer of denatured protein caused

by contact with dichloroethane. This contact denaturation of

protein has been observed in cyclic voltammetric experiments with

BSA (78) and reported for a number of different organic solvents.

The effect of CBA in this system for the above reasons is not

believed to show the effect of a dye-protein interaction although

a similar result might have been expected in the event of such an

interaction i.e. if the protein bound dye, provided the protein

had no charge, the dye charges would be shielded and the adsorption

would look like a neutral species over the entire potential range.

CHAPTER 3

CONCLUSION

     This study has shown that the use of liquid-liquid interfaces with triazinyl affinity dyes shows a great deal of promise as a means of biosensing. The dyes which have a known affinity for proteins can be modified without great effect on their physical properties and can be made to adsorb at liquid-liquid interfaces by a suitable choice of potential. Liquid-liquid interfaces provide a quick and easy method of detecting this adsorption. At present the exact nature of the adsorption is not clear. However, future work with other triazine dyes and anthracene derivatives should elucidate this problem.

     Adsorbing the dyes at a liquid-liquid interface in place of coupling them to a matrix frees the dye molecules from the steric hindrance imposed by the matrix and rigid attachment and should allow for a defined orientation of the molecules. However, the protein denaturation at the water-dichloroethane interface does provide a problem. In future work, investigation of the use of other organic solvents or to avoid direct protein-dichloroethane contact will be carried out. Other future work will include capacitance measurements of the interface in the presence of the dye to confirm the surface tension data, and to obtain more detailed information of the dye-protein affinity, analysis via Michealis-Menton or other kinetic techniques will be carried out.

     Once this work has been fulfilled it is obvious that we will have a good knowledge of the dye-protein interaction and be able to

apply this knowledge to the preparation of PTFE or PVC supported
liquid membranes for use as biosensors. Additionally, information
of the dye-protein interaction will aid research into affinity
chromatography and perhaps even protein structure elucidation.

References

1. L. Somerville and F. Quiocho, Biochim. Biophys. Acta, <u>481</u>
    (1977) 493.

2. A. Glazer, J. Biol. Chem. <u>242</u> (1967) 3326.

3. E. Rossi, E. Holler, S. Kumar, J. Rupley, G. Hess, Biochem.
    Biophys. Res. Com., <u>37</u> (1969)757.

4. A. Glazer, J. Biol. Chem., <u>242</u> (1967) 4528.

5. G. Kapperschläger, H. Böhme and E. Hofmann, Adv. Biochem.
    Eng., <u>25</u> (1982) 101.

6. Amicon manual on dye-ligand affinity chromatography.

7. Interaction of Tryptophanyl-tRNA synthetase with the triazine
    dye Brown MX-5BR. Original draft by J. McArdell, T. Atkinson
    and C. Bruton.

8. The use of triazine dyes as ligands for affinity chromatography
    of thermostable glycerokinase. Original draft by P. Hammond,
    T. Atkinson and M. Scawen.

9. G. Kopperschlager, R. Freyer and W. Diezel, FEBBS Lett. 1 (1968)
    137.

10. H. Bohme, G. Kopperschlager, J. Schultz and E. Hofmann,
    J. Chromat. <u>69</u> (1972) 209.

11. E. Stellwagen, Nature <u>257</u> (1975) 716.

12. M. Byford and D. Bloxham, Biochem. J. <u>223</u> (1984) 359.

13. J. Koryta, M. Brezina, A. Hofmanova, D. Homolka, L. Hung,
    W. Khalil, V. Marecek, Z. Samec, S. Sen, P. Vanysek,
    J. Weber, Bioelectrochem. Bioenerg. <u>7</u> (1980) 61.

14. H. Girault, D. Schiffrin, J. Electroanal. Chem. <u>179</u> (1984) 277.

15. H. Girault, D. Schiffrin, Charge and field effects in biosystems.

16. L. Berlouis, J. Chatham, H. Girault and D. Schiffrin, direct draft.

17. P. Vanysek, J. Electroanal. Chem., <u>121</u> (1981) 149.

18. J. Koryta, P. Vanysek, M. Brezina, J. Electroanal. Chem. <u>67</u>
    (1976) 263.

19. J. Koryta, P. Vanysek, M. Brezina, J. Electroanal. Chem. <u>75</u>
    (1977) 211.

20. Z. Samec, V. Mareck, J. Weber, D. Homolka, J. Electroanal.
    Chem. <u>99</u> (1979) 385.

21. H. Girault, D. Schiffrin, B. Smith, J. Colloid. Interface Sci.
    <u>101</u> (1984) 257.

22. H. Girault, D. Schiffrin, J. Electroanal. Chem. <u>137</u> (1982) 207.

23. E. Starkenstein, Biochem. Z. 24 (1910) 191.

24. R. Haekel, B. Hess, W. Hauterborn, K.H. Wuster, Z. Physiol Chem. 349 (1968) 699.

25. K. Blume, Biochim. Biophys. Acta, 227 (1971) 364.

26. D. Apps, C. Gleed, Biochem. J. 159 (1976) 441.

27. S. Thompson, E. Stellwagen, Proc. Nat. Acad. Sci. 73 (1976) 361.

28. S. Thompson, E. Stellwagen, Proc. Nat. Acad. Sci. 72 (1975) 669.

29. R. Kobayashi, V. Fang, Biochim. Biophys. Res. Com. 69 (1976) 1080.

30. A. Ashton, G. Polya, Biochem. J. 175 (1978) 501.

31. R. Beissner, F. Rudolph, J. Chromat. 161 (1978) 127.

32. E. Stellwagen, J. Mol. Biol. 106 (1976) 903.

33. E. Grazi, A.D. Iasio, G. Trombetta, E. Magri, Arch. Biochim. Biophys. 190 (1978) 76.

34. D. Watson, J. Harvey, D. Dean, Biochem. J. 173 (1978) 591.

35. D. Cottreau, M. Levin, A. Kahn, Biochim. Biophys. Acta. 568 (1979) 183.

36. R. Edwards, R. Woody, Biochim. Biophys. Res. Com. 79 (1977) 470.

37. J. Travis, R. Pannell, Clin. Chim. Acta. 49 (1973) 49.

38. J. Biellmann, J. Samama, C. Bränden, H. Eklund, Eur. J. Biochem. 102 (1979) 107.

39. R. Beissner, F. Rudolph, Arch. Biochem. Biophys. 189 (1978) 76.

40. A. Glazer, Proc. Nat. Acad. Sci. 65 (1970) 1057.

41. W. Nernst, E. Reisenfeld, Ann. Phys. 8 (1902) 600.

42. H. Sand, Ph.1. Mag. 1 (VI Series) (1901) 45.

43. J. Gustalla, J. Chim. Phys. 53 (1956) 470.

44. M. Blank, J. Colloid. Interface Sci. 22 (1966) 51.

45. C. Gavach, P. Seta, B. d'Epenoux, J. Electroanal. Chem. 83 (1977) 225.

46. Z. Samec, V. Maracek, D. Homolka, J. Electroanal. Chem. 126 (1981) 121.

47. V. Maracek, Z. Samec, J. Electroanal. Chem. 149 (1983) 185.

48. J. Reid, O. Melroy, R. Buck, J. Electroanal. Chem. 147 (1983) 71.

49. J. Reid, P. Vanysek, R. Buck, J. Electroanal. Chem. 161 (1984) 1.

50. H. Girault, D. Schiffrin, J. Electroanal. Chem. <u>170</u> (1984) 127.

51. H. Girault, D. Schiffrin, J. Electroanal. Chem. <u>150</u> (1983) 43.

52. J. Gustalla, Nature <u>227</u> (1970) 485.

53. C. Gavach, B. d'Epenoux, F. Henry, J. Electroanal. Chem. <u>64</u> (1975) 107.

54. O. Melroy, W. Bronner, R. Buck, J. Electrochem. Soc. <u>130</u> (1983) 373.

55. G. Geblewicz, Z. Koczorowsk, Z. Figaszewski, Colloids and Surfaces <u>6</u> (1983) 43.

56. Z. Koczorowski, G. Geblewicz, J. Electroanal. Chem. <u>108</u> (1980) 117.

57. D. Homolka, L. Hung, A. Hofmanova, W. Khalil, J. Koryta, V. Maracek, Z. Samec, S. Sen, P. Vanysek, J. Weber, M. Brezina, Anal. Chem. <u>52</u> (1980) 1606.

58. T. Osakai, T. Kakutani, M. Senda, Bull. Chem. Soc. Jap. <u>57</u> (1984) 370.

59. D. Homolka, V. Marecek, Z. Samec, J. Electroanal. Chem. <u>163</u> (1984) 159.

60. T. Fujinaga, S. Kihara, Z. Yoshida, Bunseki Kagaku <u>31</u> (1982) E301.

61. P. Vanysek, W. Ruth, J. Koryta, J. Electroanal. Chem. <u>148</u> (1983) 117.

62. Z. Yoshida, H. Freiser, J. Electroanal. Chem. <u>162</u> (1984) 307.

63. J. Gustalla, Mem. Serv. Chim. Etat. <u>41</u> (1956-57) 317.

64. D. Homolka, L. Hung, A. Hofmanova, W. Khalil, J. Koryta, V. Maracek, Z. Samec, S. Sen, P. Vanysek, J. Weber, M. Brezina, M. Janda, J. Stibor, Anal. Chem. Com. <u>6</u> (1975) 200.

65. Z. Samec, D. Homolka, V. Maracek, Z Kavan, J. Electroanal. Chem. <u>145</u> (1983) 213.

66. A. Watanabe, M. Matsumoto, H. Tamai, R. Gotch, Kolloid z.z. Polym. <u>220</u> (1967) 152.

67. Z. Koczorowski, G. Geblewicz, J. Paleska, J. Electroanal. Chem. <u>172</u> (1984) 327.

68. Z. Yoshida, H. Freiser, J. Electroanal. Chem. <u>162</u> (1984) 307.

69. E. Makrlik, L. Hung, A. Hofmanova, Electrochim. Acta <u>28</u> (1983) 847.

70. A. Parker, Electrochim. Acta <u>21</u> (1976) 671.

71. A. Baird and L. Faulkner, Wiley, 1980, Electrochemical Methods.

72. M. Abraham and A. Danil de Namor, J. Chem. Soc. Farad. Trans. 1 <u>72</u> (1976).

73. M. Abraham and J. Inorg. Nic. Chem. <u>43</u> (1981) 143.

74. G. Geblewicz, Personnel communication.

75. R. Stokes and R. Robinson, Butterworths, London 1959 - Electrolyte solutions.

76. H. Girault and D. Schiffrin, J. Electroanal. Chem. <u>161</u> (1984) 415.

77. Aldrich catalogue of I.R. (1984).

78. P. Vanysek, J. Reid, M. Craven and R. Buck, J. Electrochem. Soc. <u>131</u> (1984) 1788.